

1 **Running title:** OsmiR396d integrates BR and GA signaling in rice

2 **Corresponding authors:**

3 Yunyuan Xu, The Key Laboratory of Plant Molecular Physiology, Institute of Botany,
4 Chinese Academy of Sciences, Beijing 100093, China; Tel, +86 010 62836683;
5 Email: xuyy@ibcas.ac.cn.

6 Kang Chong, The Key Laboratory of Plant Molecular Physiology, Institute of Botany,
7 Chinese Academy of Sciences, Beijing 100093, China; Tel, +86 010 62836517;
8 Email: chongk@ibcas.ac.cn.

9 **OsmiR396d miRNA affects gibberellin and brassinosteroid signaling to**
10 **regulate plant architecture**

11

12 **Yongyan Tang^{#,a}, Huanhuan Liu^{#,a,b}, Siyi Guo^{a,b}, Bo Wang^{a,b}, Zhitao Li^{a,b}, Kang**
13 **Chong^{a,b}, and Yunyuan Xu^a**

14 ^a The Key Laboratory of Plant Molecular Physiology, Institute of Botany, Chinese
15 Academy of Sciences, Beijing 100093, China

16 ^b University of Chinese Academy of Sciences, Beijing 100049, China

17 [#] These authors contributed equally to the article.

18 **One sentence summary:** The microRNA396d connects OsBZR1 with OsGRFs to
19 regulate the signal of brassinosteroid and gibberellin for controlling the key
20 agriculture yield traits in rice.

21 **Author contributions:** Y.Y.X., K.C., Y.Y.T., and H.H.L. planned and designed the
22 research. Y.Y.T., H.H.L., S.Y.G., B.W., and Z.T.L. performed the experiments.
23 Y.Y.T., and H.H.L. analyzed the data. Y.Y.T., Y.Y.X., and K. C. wrote the manuscript.

24 **Funding information:** This work was supported by the National Natural Science
25 Foundation of China (91335101) and a grant from the Chinese Academy of Sciences

26 (XDA08010205).

27

28 ABSTRACT

29 Genetic improvement of plant architecture is one of the strategies for increasing the
30 yield potential of rice (*Oryza sativa*). Although great progress has been made in the
31 understanding of plant architecture regulation, the precise mechanism is still an urgent
32 need to be revealed. Here, we report that over-expression of *OsMIR396d* in rice results
33 in semi-dwarf and increased leaf angle, a typical phenotype of BR enhanced mutant.
34 *OsmiR396d* is involved in the interaction network of BR and GA signal. In *OsMIR396d*
35 over-expression plants, BR signaling was enhanced. In contrast, both the signaling and
36 biosynthesis of GA were impaired. BRASSINAZOLE-RESISTANT1 (*OsBZR1*), a
37 core transcription activator of BR signaling, directly promoted the accumulation of
38 *OsmiR396d* which controlled BR response and GA biosynthesis by regulating the
39 expression of different target genes respectively. *GROWTH REGULATING FACTOR 6*
40 (*OsGRF6*), one of *OsmiR396d* targets, participated in GA biosynthesis and signal
41 transduction, but was not directly involved in BR signaling. This study provides a new
42 insight into the understanding of interaction between BR and GA from multiple levels
43 on controlling plant architecture.

44 INTRODUCTION

45 One of the major goal for cereal crop breeding is to increase grain yields. An ideal
46 plant architecture is a concept for high grain yield in rice breeding (Khush, 2013).
47 Moderate plant height and erect leaves are two of the main factors for ideal plant
48 architecture in rice (Yuan, 2001). In the 1960s, the introduction of semi-dwarf gene *sd1*
49 greatly increased rice yields throughout Asia, and brought about the “green revolution”,
50 as a result of increased lodging resistance and harvest index in the semi-dwarf *sd1*
51 mutant (Spielmeyer et al., 2002). Leaf angle has progressively decreased due to genetic
52 improvement of *japonica* and *indica* rice cultivars in China in recent decades (Yang et
53 al., 2006; Wu et al., 2007; Hao et al., 2010). Erect leaves can capture more sunlight and
54 store more nitrogen, thus improving grain filling and increasing rice yield (Sinclair &
55 Sheehy, 1999). For example, the erect leaf rice mutant, *osdwarf4-1*, which is partially
56 deficient in biosynthesis of brassinosteroid (BR), can improve biomass production and

57 grain yield under dense planting conditions without extra fertilizer (Sakamoto et al.,
58 2006).

59 Gibberellin (GA) and brassinosteroid (BR) are two predominant plant hormones that
60 determine plant height and leaf angle by regulating cell growth (Tong et al., 2014;
61 Zhang et al., 2014). GA is perceived and bound by the soluble protein GIBBERELLIN
62 INSENSITIVE DWARF1 (GID1), which results in GID1 conformation change, thus
63 the interaction of GID1 and DELLA proteins (GA response repressors) is promoted
64 (Ueguchi-Tanaka et al., 2007; Hedden & Sponsel, 2015). The GA-GID1-DELLA
65 complex recruits an F-box protein (SLY1 in *Arabidopsis* and GID2 in rice), and
66 subsequently DELLA is ubiquitinated by SCF E3 ubiquitin ligase and then degraded
67 through the proteasomal degradation pathway. Following this, GA signal transduction
68 is released from repression by DELLA proteins and cell elongation is promoted
69 (McGinnis et al., 2003; Sasaki et al., 2003; Hirano et al., 2010).

70 BR signal transduction pathway is mainly shared in *Arabidopsis* and rice (Zhang et
71 al. 2014). BR is perceived by leucine-rich repeat receptor-like kinases
72 BRASSINOSTEROID-INSENSITIVE 1 (BRI1) and its co-receptor
73 BRI1-ASSOCIATED RECEPTOR KINASE 1 (BAK1) (Clouse et al., 1996;
74 Yamamuro et al., 2000; Li et al., 2002; Wang, et al., 2008). Then, the signal is passed
75 along to a key negative regulator, BRASSINOSTEROID-INSENSITIVE 2 (BIN2),
76 which is dephosphorylated by BRI1 SUPPRESSOR 1 (BSU1) (Li et al., 2001;
77 Mora-Garcia et al., 2004; Kim et al., 2011). In rice, the dephosphorylation of
78 GSK3/SHAGGY-like Kinase (OsGSK2) (a rice homolog of *Arabidopsis* BIN2)
79 releases its suppression on BRASSINAZOLE-RESISTANT1 (OsBZR1), LEAF AND
80 TILLER ANGLE INCREASED CONTROLLER (OsLIC), DWARF AND
81 LOW-TILLERING (OsDLT), OVATE Family Protein 8 (OsOFP8) and REDUCED
82 LEAF ANGLE1 (RLA1) to activate BR response and increase leaf angle (Bai et al.,
83 2007; Wang, L et al., 2008; Tong et al., 2009; Tong et al., 2012; Zhang et al., 2012;
84 Yang et al., 2016, Qiao et al., 2017). The kinase activity of OsGSK2 can also be directly
85 inhibited by membrane protein GW5 (QTL for grain width and weight on chromosome
86 5), which is a calmodulin-binding protein (Liu et al., 2017).

87 The crosstalk network between BR and GA is quite complicated. BR and GA
88 interact not only at biosynthesis regulation level, but also at signaling level. And their
89 crosstalk differs depending on hormone concentrations, development stages, tissues
90 and species (Tong & Chu, 2016; Unterholzner et al., 2016). BR signaling defected
91 mutants are impaired in GA biosynthesis in *Arabidopsis* and rice (Tong et al., 2014;
92 Unterholzner et al., 2015). Expression of GA biosynthesis gene *GA20ox1* under the
93 promoter of *BRI1* in *bri1-301* mutant can rescue most of its defects (Unterholzner et al.,
94 2015). *Arabidopsis* BES1 and rice OsBZR1 can bind the promoters of GA biosynthesis
95 or inactivation genes to regulate GA biosynthesis (Tong et al., 2014; Unterholzner et
96 al., 2015). On the other hand, GA regulates BR biosynthesis at transcription level.
97 OsSPY, a negative regulator of GA signaling, negatively regulates BR biosynthesis
98 (Shimada et al., 2006). OsGSR1, a positive regulator of GA signaling, activates BR
99 synthesis by directly interacting with BR biosynthesis enzyme, DWF1 (Wang et al.,
100 2009). There is also a physical interaction between BR and GA at the signaling level.
101 The GA signaling negative regulator, DELLA protein, interacts with BZR1/BES1 and
102 inhibits their function. Thus GA can release the inhibition of DELLA on BZR1/BES1
103 to induce downstream BR responses in *Arabidopsis* (Bai et al., 2012;
104 Gallego-Bartolome et al., 2012; Li et al., 2012). Although, great progresses have been
105 made in this aspect, the knowledge we get now is far from enough to understand the
106 interaction network of BR and GA. More related research work need to be carried out.

107 MicroRNAs (miRNAs) also participate in hormone regulation and plant
108 development, especially in integrating distinct agricultural traits (Tang & Chu, 2017).
109 miR396 represents one of the most deeply conserved miRNA families in plants (Liu et
110 al., 2009). Many studies have been performed in *Arabidopsis* and rice focusing on
111 miR396 and its targets, *GROWTH REGULATING FACTORS (GRFs)*. In rice,
112 OsmiR396 and its targets, *OsGRFs*, regulate leaf development, plant height, meristem
113 function, flowering time, inflorescence architecture, and seed size (Luo et al., 2005;
114 Kuijt et al., 2014; Liu et al., 2014; Che et al., 2015; Duan et al., 2015; Gao et al., 2015).
115 OsGRF4 interacts with OsGIFs to control seed size through BR signaling, and its
116 transcription activity can be directly regulated by OsGSK2 (Che et al., 2015; Duan et
117 al., 2015). OsGRF6 is involved in floral organogenesis by regulating the expression of

118 *JMJD2* family *jmjC* gene 706 (*OsJMJ706*) and *Crinkly4* receptor-like Kinase (*OsCR4*)
119 (Liu et al., 2014). *OsGRF6* also modulates inflorescence architecture through the IAA
120 regulating pathway (Gao et al., 2015).

121 It is well established that *OsmiR396* targets *OsGRFs* to function in the regulation
122 pathway of multiple hormones such as GA, BR, and auxin (van der Knaap et al., 2000;
123 Che et al., 2015; Gao et al., 2015). However, little is known about how *miR396* is
124 regulated in plant development. Here, we show that *OsmiR396d* is involved in the BR
125 signaling transduction pathway and is directly activated by the key transcription factor
126 *OsBZR1*. *OsmiR396d* also participates in the regulation of GA signaling by
127 modulating the expression of *OsGRF6*, which is independent of BR signaling. Our
128 findings reveal that the *OsmiR396d* can combine the BR and GA regulation pathway to
129 control rice plant architecture.

130

131 **RESULTS**

132 **Over-expression of *OsMIR396d* changed rice plant architecture**

133 Our previous study showed that *OsMIR396d* over-expression transgenic plants
134 (miROE) exhibited abnormal florets. *OsmiR396d* target genes, *OsGRF6* and
135 *OsGRF10*, were involved in regulating floral organ identity and husk opening (Liu et
136 al., 2014). In miROE lines, the third leaf angles were increased to two times more than
137 that of Zhonghua 10 (ZH10) at the seedling stage (Fig. 1A, B). The increased leaf angle
138 phenotype was also observed on the top three leaves of miROE lines at the seed filling
139 stage (Fig. 1B). miROE8 had the highest expression level of *OsmiR396d* among the
140 transgenic lines (Liu et al., 2014) and exhibited the largest leaf angle. The angles of top
141 third leaf of ZH10, miROE2, miROE5, miROE8, and miROE10 were 17°, 29°, 30°,
142 36°, and 32° respectively (Fig. 1B).

143 The height of miROE plants was also significantly decreased compared with ZH10
144 (Fig. 2A). The data showed that the plant height of miROE was only 70-80% of that of
145 ZH10, and every internode of miROE was shortened compared with ZH10 (Fig. 2B, C).
146 The fifth internode of miROE exhibited severe growth retardation in particular (Fig.
147 2D). The fifth internode length was decreased from 2.6 cm in ZH10 to about 1.0 cm in
148 miROE lines. The relative lengths of each internode (percentage of each internode
149 length to total culm length) had no obvious differences between miROE and ZH10,
150 except that the fifth internode was reduced from 2.6% in ZH10 to about 1.5% in
151 miROE (Fig. 2E).

152 **The collar adaxial cell size was enlarged in *OsMIR396d* over-expression plants**

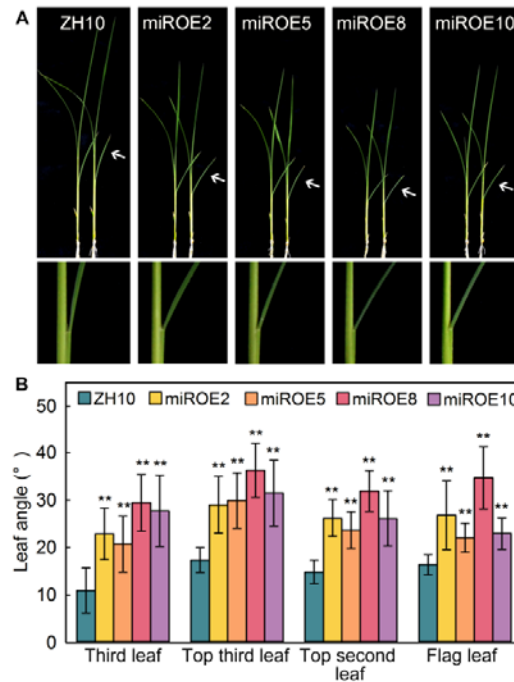


Figure 1. The leaf angle of *OsMIR396d* over-expression plants was increased.

A. The third leaf angle of miROEs was specifically increased. Bar = 1 cm.

B. Statistical analysis of leaf angles. The third leaf angle was measured at the seedling stage and the angles of the top three leaves were measured at the seed filling stage. Error bars indicate SD for at least fifteen plants. Asterisks indicate $P < 0.01$ (**) compared with wild type in the Student's t test analysis.

153 The promotion of lamina inclination is one of the most typical BR responses in rice,
 154 and it is often caused by proliferation or expansion of collar adaxial cells (Wada et al.,
 155 1981; Cao & Chen, 1995; Sun et al., 2015). To determine the cell structure basis for
 156 increased leaf angle of miROE, the adaxial surface and longitudinal sections of
 157 miROE8 and ZH10 lamina joints were observed using scanning electron microscopy
 158 (SEM). The lamina joint adaxial side of miROE8 was obviously expanded compared to
 159 ZH10 (Fig. 3A, D), and the cell size in the adaxial region of miROE8 was much larger
 160 than that of ZH10 (Fig. 3B, C, E, F). Especially, miROE8 cells were expanded nearly
 161 one fold larger than ZH10 along the proximal-distal axis (Fig. 3G). In contrast, the cell
 162 layers in the lamina joint adaxial side were not distinct between miROE8 and ZH10 at
 163 both proximal-distal axis (half frame indicated regions in Fig. 3B and E) and
 164 adaxial-abaxial axis. Therefore, these results indicated that the increased leaf angle of
 165 miROE might mainly result from enlarged cell size at the adaxial side of the lamina
 166 joint.

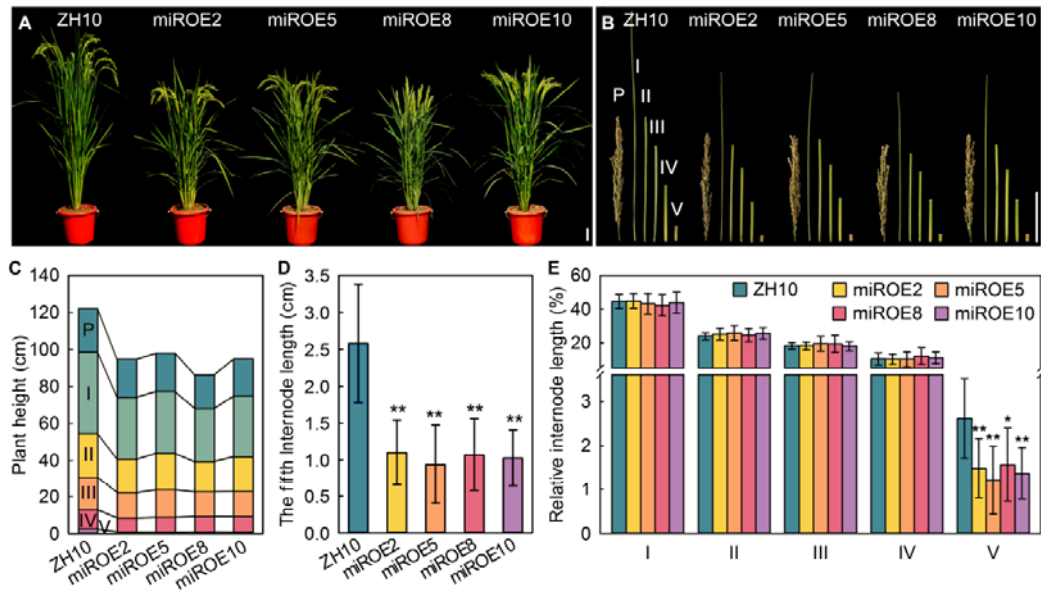


Figure 2. The plant height and length of internodes in *OsMIR396d* over-expression plants were reduced.

A. The phenotype of miROEs and ZH10 at the seed filling stage. Bar = 5 cm.

B. The panicle and internodes of miROEs and ZH10. Bar = 5 cm.

C. Results of statistical analysis of plant height and internode length of miROE lines and ZH10. More than fifteen mature plants were used in each analysis.

D. Results of statistical analysis of fifth internode lengths of miROEs and ZH10. Error bars indicate SD for at least fifteen plants. Asterisks indicate $P < 0.01$ (**) compared with ZH10 in the Student's t test analysis.

E. Relative internode length of miROEs and ZH10. The data shows each internode length relative to the total culm length. Error bars indicate SD for at least fifteen plants. Asterisks indicate $P < 0.05$ (*) and $P < 0.01$ (**) compared with ZH10 in the Student's t test analysis.

167 Cell elongation and division were arrested in *OsMIR396d* over-expression plants

168 To figure out the reason for the semi-dwarf phenotype of miROE plants, the cell
 169 sizes in the second leaf sheaths were analyzed. Compared with ZH10, the cell length of
 170 miROE8 was slightly decreased (Fig. 4A, B). In addition, the cell cycle progression
 171 was analyzed by flow cytometry using root apical cells. The results showed that the
 172 DNA content of miROE8 was decreased compared to ZH10 (Fig. 4C). Thus, miROE
 173 possessed fewer cells in the G2/M phase. The mitotic index, a measure for the
 174 proliferation status of a cell population (Simpson et al., 1992), was about 9.4% in
 175 miROE8, which was significantly lower than that of ZH10 (16.4%) (Fig. 4D).
 176 Therefore, the semi-dwarf phenotype of miROE plants was caused by both impaired
 177 cell elongation and reduced cell division.

178 *OsmiR396d* is involved in the BR signaling pathway

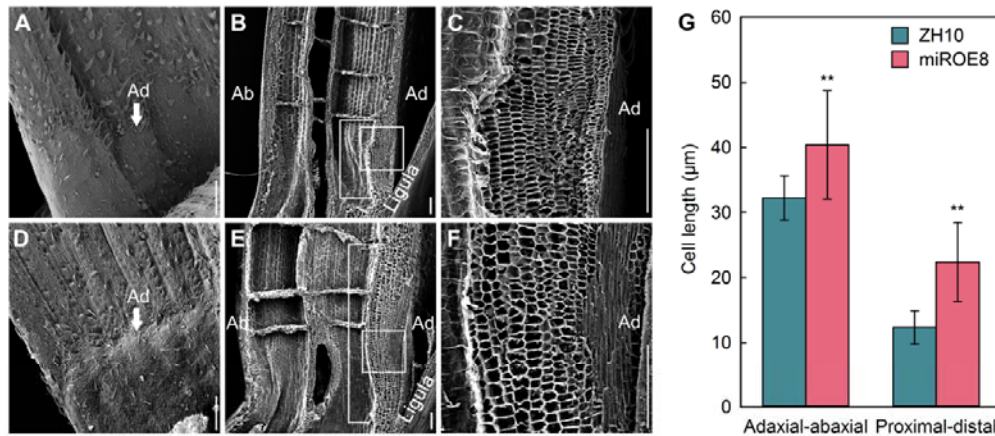


Figure 3. Scanning electron microscopic examination of the leaf lamina joint.

A, B. Adaxial surface of the leaf lamina joint in ZH10 (A) and miROE8 (B). Arrows indicate the increased growth of cells.

C, D. Longitudinal sections of the leaf lamina joint of ZH10 (C) and miROE8 (D). Half frame indicated regions were used to calculate cell layers.

E, F. Close-up of regions denoted by rectangles in (C) and (D) respectively. Ad, adaxial; Ab, abaxial. Scale bars = 200 μm.

G. Statistical analysis of cell length in (C) and (F). Cell length along the adaxial-abaxial axis and proximal-distal axis were measured respectively. Error bars indicate SD for at least 100 cells. Asterisks indicate $P < 0.01$ (**) compared with ZH10 in the Student's *t* test analysis.

179 The increased leaf angle and semi-dwarf phenotypes of miROE plants are similar
 180 to the phenotypes of BR signal-enhanced rice plants, such as *OsLIC* antisense lines
 181 (Zhang et al., 2012) and *ili1-D* mutant (Zhang et al., 2009). Therefore, it is possible that
 182 OsmiR396d is involved in positive regulation of BR signaling. To investigate this
 183 possibility, the effects of OsmiR396d on BR signaling were examined by leaf angle and
 184 root length growth of miROE8 and ZH10 in the presence of 24-epibrassinolide
 185 (24-eBL). The leaf angle of miROE8 was increased more efficiently than that of ZH10
 186 when exogenous 24-eBL was applied (Fig. 5A). The root growth of miROE8 was also
 187 more sensitive to 24-eBL compared to ZH10 (Fig. 5B). These 24-eBL treatment results
 188 implied that OsmiR396d positively regulated BR signaling in rice. To figure out the
 189 points of BR signaling impacted with *OsMIR396d* over-expression, the expression
 190 levels of several BR regulation related genes were compared between miROEs and
 191 ZH10. The qRT-PCR result showed that the positive regulatory genes of BR signaling,
 192 *OsBR11* and *OsDLT1*, were upregulated in miROEs, while the negative regulatory gene
 193 of BR signaling *OsLIC* was downregulated (Supplemental Fig. S1). This result
 194 indicated that OsmiR396d might regulate multiple steps of the BR signaling pathway.

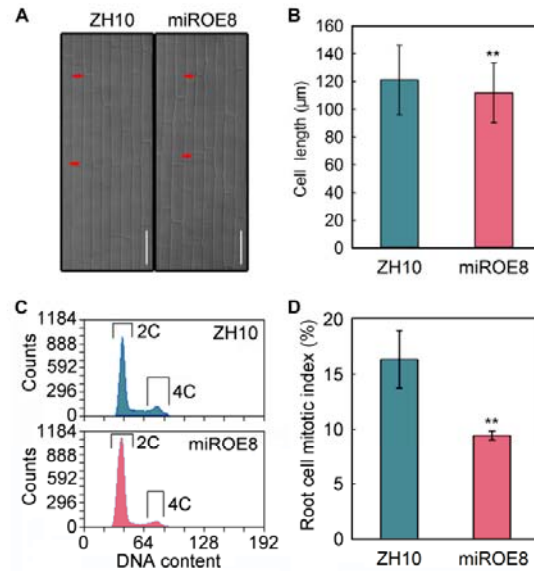


Figure 4. Cell length and cell division analysis.

A. The second leaf sheath cells of 2-week-old seedlings of miROE8 and ZH10. Bars = 50 μm .

B. The statistical analysis of cell length in the second leaf sheath. Error bars indicate SD for more than 400 cells. Asterisks indicate $P < 0.01$ (**) compared with ZH10 in student's t test analysis.

C. The DNA content of miROE8 and ZH10. After the seeds germinated for 3 days at 28°C, the root tips were harvested. Cell nuclei (10,000) were stained with 1 $\mu\text{g mL}^{-1}$ DAPI and analyzed by flow cytometry. 2C and 4C represent the DAPI signals that correspond to nuclei with different DNA contents.

D. Cell mitotic index in root apical meristem in miROE8 and ZH10. The results were from three independent replications. Error bars indicate SD. Asterisks indicate $P < 0.01$ (**) compared with ZH10 in the Student's t test analysis.

195 How BR influences *OsMIR396d* expression was also investigated. The response of
 196 *OsMIR396d* to 24-eBL was detected by qRT-PCR. Compared with the control, the
 197 expression level of *OsMIR396d* was upregulated under 24-eBL treatment and reached
 198 the highest level after treatment for 3 h (Fig. 5C). Consistently, the transcript level of
 199 several *OsGRFs* decreased after BR treatment for 3 h (Supplemental Fig. S2).
 200 Furthermore, the expression level of *OsMIR396d* in BR signaling enhanced or impaired
 201 rice plants was checked. The qRT-PCR results showed that the expression of
 202 *OsMIR396d* was increased in the BR-signal enhanced *OsLIC* antisense line (LIC-AS)
 203 (Zhang et al., 2012) and the *OsBZR1* over-expression line (BZR1-OE), but decreased in
 204 the BR-signal reduced *OsBZR1* RNAi line (BZR1R) (Bai et al., 2007) (Fig. 5D). These
 205 results indicated that *OsMIR396d* transcription was induced by both exogenous BR
 206 treatment and endogenous BR signal.

207 ***OsMIR396d* is a direct target of OsBZR1**

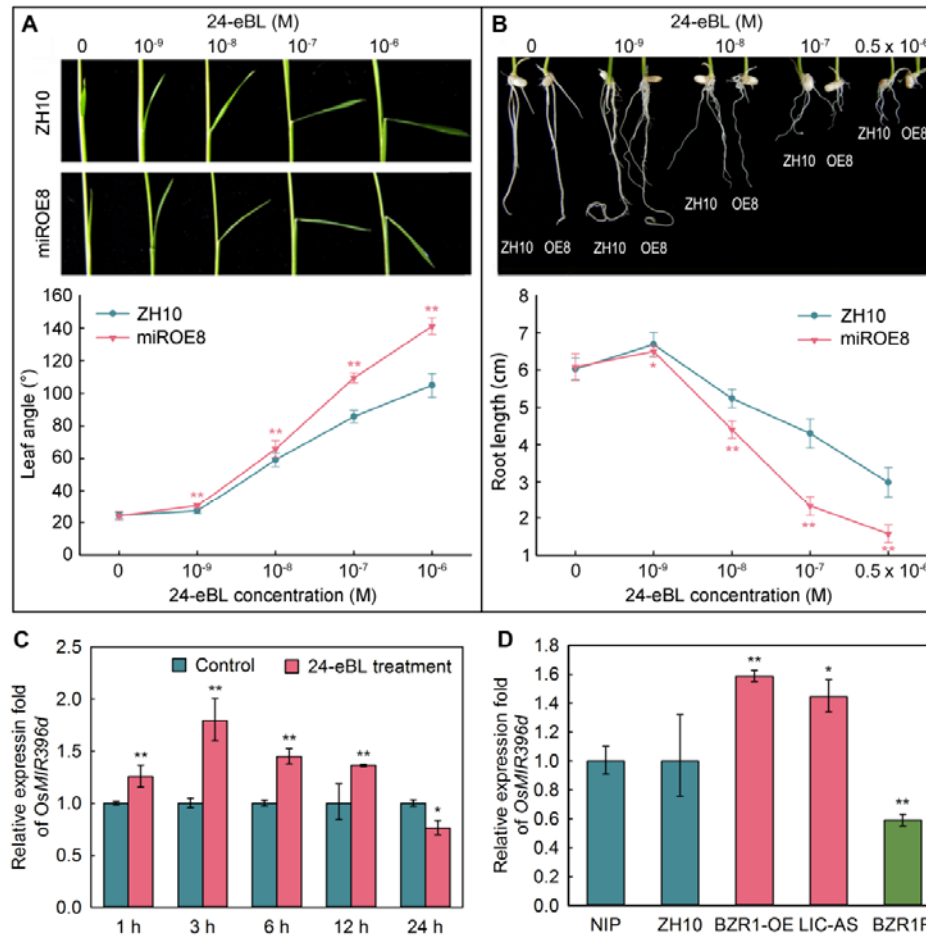


Figure 5. OsMIR396d is involved in BR signaling.

A. Lamina joint inclination assay of miROE8 and ZH10. The second lamina joints of one-week-old seedlings grown under dark condition were cut off and treated with different concentrations of 24-eBL for three days. Error bars indicate SD for at least fifteen plants. Asterisks indicate $P < 0.05$ (*) and $P < 0.01$ (**) compared with ZH10 in the Student's t test analysis.

B. The seminal root growth of miROE8 and ZH10 under treatment with different concentrations of 24-eBL. The seminal root length was measured after seedlings were grown in 24-eBL containing 1/2 MS medium for one week. Error bars indicate SD for at least fifteen plants. Asterisks indicate $P < 0.05$ (*) and $P < 0.01$ (**) compared with ZH10 in the Student's t test analysis.

C. The expression pattern of OsMIR396d under treatment with 24-eBL. Two-week-old ZH10 seedlings were treated with 1 μ M 24-eBL. Whole plants were sampled 1, 3, 6, 12 and 24 h after treatment. The plants sampled from the normal growth condition were used as control. *UBQUITIN1* was used as a reference gene. Error bars indicate SD for three replicates. Asterisks indicate $P < 0.05$ (*) and $P < 0.01$ (**) compared with control in the Student's t test analysis.

D. The expression of *OsMIR396d* in *OsLIC* antisense plants (LIC-AS), *OsBZR1* RNAi plants (BZR1R), and *OsBZR1* over-expression (BZR1-OE) plants. LIC-AS and BZR1R were under the background of ZH10 and BZR1-OE was under the background of Nipponbare (NIP). *UBQUITIN1* was used as reference gene. Error bars indicate SD for three replicates. Asterisks indicate $P < 0.05$ (*) and $P < 0.01$ (**) compared with wild-type ZH10 or NIP respectively in the Student's t test analysis.

208 The expression of *OsMIR396d* was upregulated in BZR1-OE plants and

209 downregulated in BZR1R lines (Fig. 5D). It was reported that transcription factor

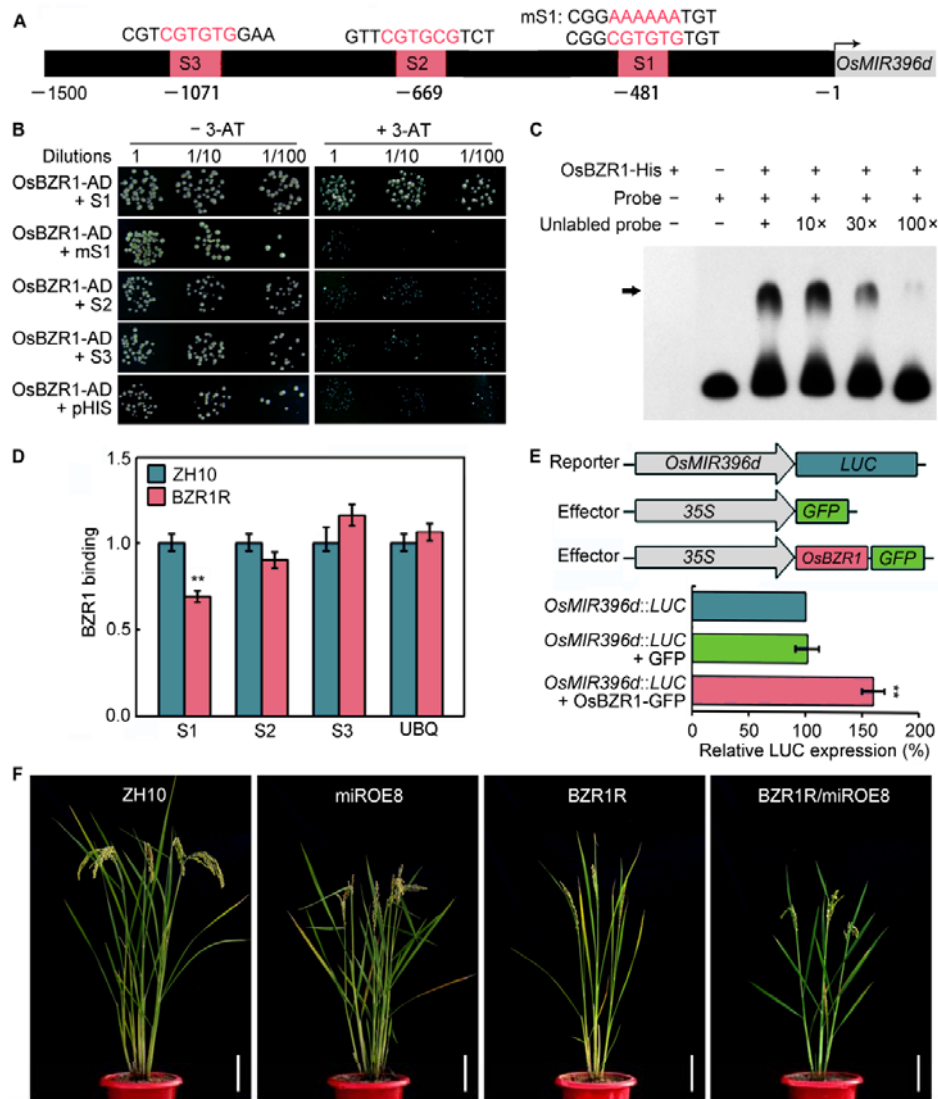


Figure 6. OsBZR1 directly activates the expression of *OsMIR396d*.

A. Localization of three putative OsBZR1 binding sites S1, S2, and S3 in the *OsMIR396d* promoter.

B. Yeast one-hybrid analysis of OsBZR1 binding the promoter of *OsMIR396d*. Empty pHIS vector was used as negative control.

C. EMSA analysis of OsBZR1 binding the promoter of *OsMIR396d*. S1-containing DNA fragment was labeled with biotin. The arrow indicates the complex of OsBZR1-His and the DNA probe.

D. ChIP-qPCR analysis of OsBZR1 binding the promoter of *OsMIR396d* using OsBZR1 antibody to enrich DNA. The UBIQUITIN DNA fragment was used as an internal control. Error bars indicate SD for three replicates. Asterisks indicate $P < 0.01$ (**) compared with ZH10 in the Student's *t* test analysis.

E. Transactivation assay of OsBZR1 with the luciferase reporter system. Error bars indicate SD for three replicates. Asterisks indicate $P < 0.01$ (**) compared with control in the Student's *t* test analysis.

F. The phenotype of OsBZR1 RNA interference transgenic plants (miROE8/*BZR1R*) under the background of miROE8. Bar = 10 cm.

210 BZR1 binds to CGTGT/CG element (He et al., 2005; Zhang et al., 2012). The 1.5 kb

211 sequence of the *OsMIR396d* promoter was screened, and three putative BZR1 binding
212 sites were found at -479 (S1), -667 (S2), and -1069 (S3) bp upstream of the
213 pre-miR396d transcription start site (Fig. 6A). These results implied that *OsMIR396d* is
214 potentially targeted by the transcription factor OsBZR1.

215 To test the direct regulation of OsBZR1 to *OsMIR396d*, yeast one-hybrid assay was
216 carried out. The data showed that OsBZR1 could bind the S1 site but not the S2 or S3
217 site. The mutation of S1 sites led to disappeared binding ability (Fig. 6B). The EMSA
218 assay further confirmed this possibility. The His-tagged OsBZR1 protein could
219 physically bind the S1 site containing DNA fragment *in vitro*, and the excess unlabeled
220 competitive probe could effectively inhibit the biotin probe bound by OsBZR1 (Fig.
221 6C). Furthermore, OsBZR1 bound the promoter of *OsMIR396d in vivo* was analyzed
222 through ChIP-qPCR via the antibody against OsBZR1. The S1-containing DNA
223 fragment was significantly decreased in BZR1R plants compared with ZH10, while the
224 amount of S2 and S3-containing DNA fragments was not significantly different
225 between BZR1R and ZH10 (Fig. 6D). In addition, activity of luciferase was used as a
226 reporter to detect the effect of OsBZR1 on *OsMIR396d* expression in *Arabidopsis*
227 protoplasts. The data showed that the luciferase activity of *OsMIR396d::LUC*
228 transfected protoplasts was increased when OsBZR1-GFP was co-expressed (Fig. 6E).
229 This result suggested that OsBZR1 positively regulates the expression of *OsMIR396d*.

230 To explore the genetic relationship of *OsMIR396d* and *OsBZR1*, the *OsBZR1* RNAi
231 vector was transformed into miROE8 to get double transgenic plants
232 (BZR1R/miROE8) (Supplemental Fig. S3). The leaf angle of BZR1R/miROE8 was
233 increased compared with BZR1R or ZH10 (Fig. 6F; Supplemental Fig. S4A, B). This
234 result suggested that the function of OsBZR1 might be partially dependent on
235 *OsMIR396d*. Additionally, miROE8 was crossed with BR receptor *OsBRI1* mutant *d61*
236 (Nakamura et al., 2006). The leaf angles were significantly increased in the progenies
237 of miROE8/*d61* compared with the parents (Supplemental Fig. S4). This result further
238 confirmed that *OsMIR396d* was involved in the BR signal regulated leaf angle
239 development process. These biochemical and genetic evidences indicate that
240 *OsMIR396d* was one direct target gene of OsBZR1.

241 **OsmiR396d is involved in the GA regulation pathway**

242 The *OsmiR396d* over-expression plants displayed decreased internode length,
243 especially the shortened fifth internode (Fig. 2). This characteristic was similar to GA
244 deficient mutants such as *d18*, *d35*, and *sd1* (Itoh et al., 2004). The cross progenies
245 miROE8/*d61* showed not only increased leaf angle but also reduced plant height
246 compared with their parents (Supplemental Fig. S4). These phenotypes implied that
247 OsmiR396d was possible to control plant height through GA signaling in addition to
248 the BR-dependent pathway.

249 To examine if OsmiR396d controls plant height through GA signaling, the GA
250 sensitivity of miROEs was analyzed by measuring the second leaf sheath length under
251 GA treatment. The results showed that the second leaf sheath length of both miROE8
252 and ZH10 were distinctly elongated under GA treatment (Fig. 7A). However, by
253 comparison, the leaf sheath of miROE8 was less sensitive to GA₃ than that of ZH10.
254 The expression levels of GA signaling and biosynthesis related genes were also
255 checked in miROEs and ZH10. Results from qRT-PCR showed that the transcription
256 levels of GA signaling pathway gene *OsGID2* and several GA biosynthesis pathway
257 genes (including *OsCPS1*, *OsKO2*, *OsGA20ox1*, and *OsGA20ox3*) were apparently
258 reduced in miROEs compared with ZH10 (Fig. 7B). The expression pattern of
259 *OsmiR396d* after treatment with paclobutrazol (PAC, GA biosynthesis inhibitor) or
260 GA₃ was also analyzed in ZH10 seedlings. The result showed the expression of
261 *OsmiR396d* was typically repressed by continuous PAC treatment, but was
262 upregulated after treatment with a high concentration of GA₃ (Supplemental Fig. S5).
263 These findings suggested that OsmiR396d participates in the GA signaling pathway
264 and regulates internal GA biosynthesis as well.

265 **OsmiR396d targeted *OsGRF6* to regulate the GA pathway**

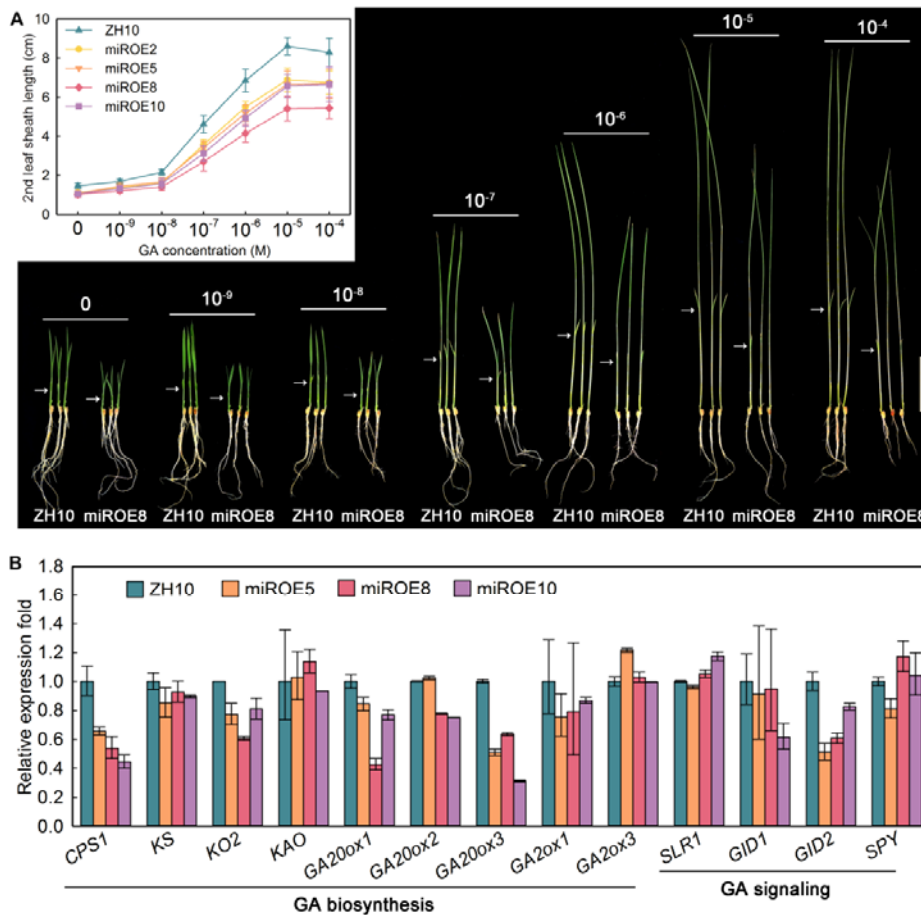


Figure 7. GA signaling and biosynthesis were impaired in *OsMIR396d* over-expression plants.

A. The phenotype of miROE8 and ZH10 seedlings growth under different concentrations of GA₃ treatment. The seeds were treated with 10 μM PAC for 2 days before cultivation in nutrient solution containing the indicated concentration of GA₃. After 10 days of growth, the seedlings were photographed. The measurements of the second leaf sheath are shown. Error bars indicate SD for at least fifteen plants. Bar = 5 cm.

B. The expression of GA pathway related genes in miROE and ZH10. *UBQUITIN1* was used as reference gene. Error bars indicate SD for three replicates.

266 *GRFs* are predicted to be the targets of miR396 (Jones-Rhoades & Bartel, 2004; Wu
 267 et al., 2009). *OsGRF6*, one target of OsmiR396d, was involved in floral organogenesis
 268 under the regulation of OsmiR396d (Liu et al., 2014). We were also interested in
 269 determining whether *OsGRF6* participates in BR and GA signaling in a similar manner
 270 as *OsMIR396d*. Our previous data showed that the plant height of *osgrf6* mutant was
 271 decreased compared with wild type Dongjin (DJ) (Liu et al., 2014). *OsGRF6* antisense

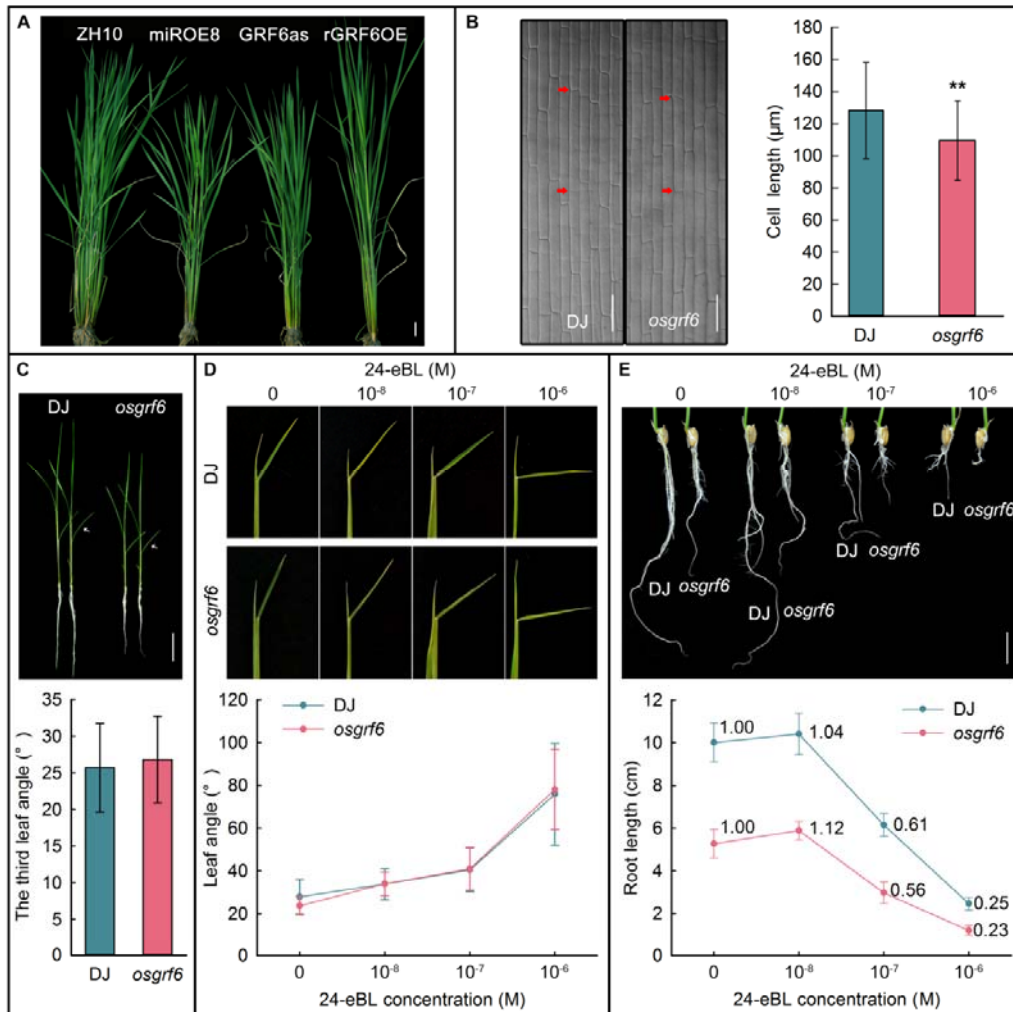


Figure 8. BR signaling was not affected in *osgrf6* mutant.

A. The phenotype of *OsGRF6* antisense transgenic plant (GRF6as) and the OsmiR396d-resistant form of *OsGRF6* transgenic plant (rGRF6OE). Bar = 5 cm.

B. The second leaf sheath cells of 2-week-old seedlings of *osgrf6* and DJ. The cell length was measured. Error bars indicate SD for more than 400 cells. Asterisks indicate $P < 0.01$ (**) compared with DJ in the Student's *t* test analysis. Bar = 50 μm .

C. The leaf angle of *osgrf6* was not changed. The third leaf angle was measured. Error bars indicate SD for at least fifteen plants.

D. Lamina joint inclination assay of *osgrf6* and DJ. Error bars indicate SD for at least fifteen plants.

E. The seminal root growth of miROES and ZH10 under treatment with different concentrations of 24-eBL. Error bars indicate SD for at least fifteen plants.

272 transgenic plants (GRF6as) were also moderately reduced compared with wild type
 273 (ZH10) plants, while the OsmiR396d-resistant form of *OsGRF6* transgenic plants
 274 (rGRF6OE) had a slightly increased plant height (Fig. 8A). Microscopy data further
 275 showed that the cell length of the *osgrf6* second leaf sheath was significantly shortened

276 compared with DJ (Fig. 8B). In contrast, the leaf angle of *osgrf6* was very similar to DJ
277 (Fig. 8C). These results suggested that OsmiR396d might target *OsGRF6* to regulate
278 plant height but nearly not affect leaf angle.

279 In lamina inclination assay, the result showed that the sensitivity of *osgrf6* to 24-eBL
280 was not apparently different from that of DJ (Fig. 8D). In seminal root growth
281 experiment, the root length of *osgrf6* mutant was much shorter than that of DJ under
282 normal growth condition, so we used relative root length to do the analysis following
283 the method used by Tong et. al (2014), and the root length under normal growth
284 condition was used as reference. The relative root length of *osgrf6* was 0.56 and that of
285 DJ was 0.61 at 10^{-7} M 24-eBL (Fig. 8E). This result also showed that there was no
286 apparent distinction in BR sensitivity between *osgrf6* and DJ. Above results indicated
287 that *OsGRF6* might not be directly involved in the BR signaling mediated lamina joint
288 development and root growth processes.

289 To determine if *OsGRF6* participates in GA regulation, *osgrf6* and DJ seeds were
290 pretreated with 10^{-5} M PAC (to inhibit endogenous GA biosynthesis) or water (control)
291 for 2 days. Then the germinated seeds were planted in nutrient solution containing 10^{-5}
292 M PAC and/or 10^{-5} M GA₃ as indicated in the Fig. 9A. The second leaf sheath of *osgrf6*
293 was significantly shorter than DJ after the treatment for 10 days. When treated only
294 with PAC, there was no difference in second leaf sheath length between *osgrf6* and DJ.
295 However, this difference appeared again when GA₃ was added into the nutrient solution
296 (Fig. 9A, B). This result implied that GA signaling or biosynthesis was likely impaired
297 in *osgrf6*. The reduced sensitivity of *osgrf6* to GA₃ was further confirmed by treating
298 *osgrf6* and DJ with different concentration of exogenous GA₃ (Supplemental Fig. S6).
299 The genes that were downregulated in miROEs were also analyzed in *osgrf6*. Results
300 from qRT-PCR showed that the expression levels of *OsCPS1*, *OsGA20ox1*,
301 *OsGA20ox3* and *OsGA3ox2* were also downregulated in *osgrf6* compared with DJ (Fig.
302 9C).

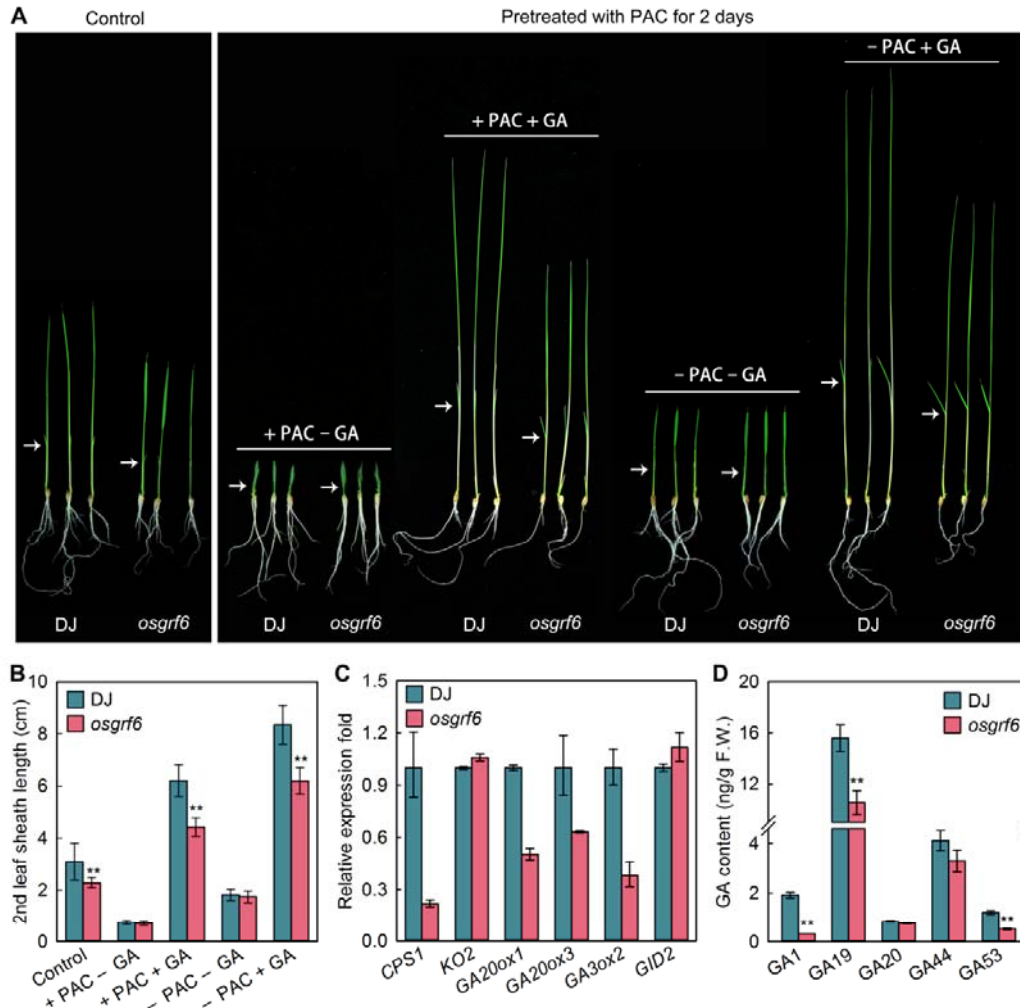


Figure 9. GA signaling and biosynthesis are impaired in the *osgrf6* mutant.

A. *osgrf6* and DJ seedlings treated with PAC or GA₃. The seeds were treated with water (control) or 10⁻⁵ M PAC for 2 days, and then germinated seeds were planted in PAC and/or GA₃ containing culture solution for 10 days. Bar = 5 cm.

B. The statistical result of the second leaf sheath length of *osgrf6* and DJ grown under PAC and/or GA₃ treatment. Error bars indicate SD for at least fifteen plants. The relative leaf sheath length between DJ and *osgrf6* was calculated and shown. Asterisks indicate P < 0.01 (**) compared with DJ in student's t test analysis.

C. The expression of GA pathway related genes in *osgrf6* and DJ. *UBQUITIN1* was used as reference gene. Error bars indicate SD for three replicates.

D. Quantification of endogenous GAs in *osgrf6* and DJ. Two-week-old seedlings were sampled. Error bars indicate SD for three replicates. Asterisks indicate P < 0.01 (**) compared with DJ in the Student's t test analysis.

303 To confirm that GA biosynthesis was impaired in *osgrf6*, endogenous GAs were
 304 quantified. The results showed that GA₁, GA₁₉, and GA₅₃ level were significantly
 305 decreased in *osgrf6* (Fig. 9D). These results demonstrated that *OsGFR6* was involved
 306 in the regulation of both GA signaling and biosynthesis.

308 **DISCUSSION**

309 BR and GA are vital hormones in plant that influence various developmental
310 processes, such as cell division, cell elongation, flowering, leaf senescence, and seed
311 germination (Greenboim-Wainberg et al., 2005; Vriet et al., 2013; Fariduddin et al.,
312 2014; Sakata et al., 2014; Hedden & Sponsel, 2015). BR and GA interact with each
313 other at both biosynthesis level and signaling level to form a potential complex network
314 (Wang et al., 2009; Zhang et al., 2012). Here, we report that *OsmiR396d* participates in
315 this interaction network of BR and GA. *OsBZR1*, as a node of BR signaling pathway,
316 can directly activate the expression of *OsMIR396d* to repress the expression of
317 *OsGRF6* for regulating GA signaling and biosynthesis (Fig. 10).

318 ***OsBZR1* targets *OsMIR396d* to control leaf angle through *OsGRF4* mediated BR**
319 **response**

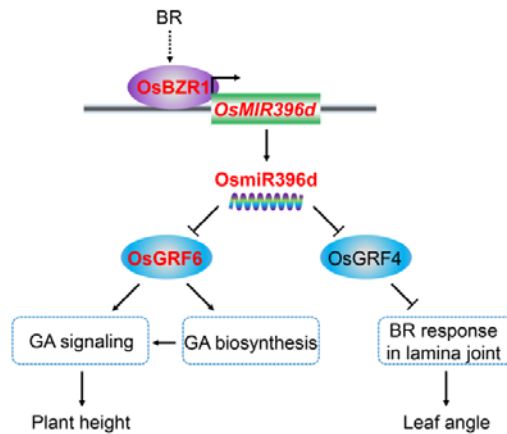


Figure 10. A proposed model for OsmiR396d controlling rice plant architecture. *OsMIR396d* is activated by OsBZR1, which is the key regulator transcription factor of BR signaling. On the right side, OsmiR396d regulates leaf angle by repressing the expression of *OsGRF4*. On the left side, OsmiR396d is involved in GA signaling and biosynthesis by regulating the expression of *OsGRF6* to control rice plant height.

320 In this study, we propose that OsmiR396d is involved in the BR signaling pathway
 321 based on data with four lines. Firstly, over-expression of *OsMIR396d* in rice resulted in
 322 increased leaf angle and semi-dwarf phenotype (Fig. 1, 2), which was similar to the
 323 phenotype of rice plants with accumulated BR or with enhanced BR signal (Tanaka et
 324 al., 2009; Tong et al., 2009; Zhang et al., 2009; Tong et al., 2012; Zhang et al., 2012).
 325 Secondly, we demonstrated that the CGTGT/CG element in the *OsMIR396d* promoter
 326 was directly bound by OsBZR1 using yeast one-hybrid experiment and EMSA assay *in*
 327 *vitro*, also ChIP-qPCR detection *in vivo*. The results of the luciferase reporter assay
 328 indicated that OsBZR1 could activate *OsMIR396d* expression (Fig. 6). Coincidentally,
 329 the *OsMIR396d* transcript level was increased in *OsBZR1* over-expression plants, but
 330 was decreased in *OsBZR1* RNAi plants (Fig. 5D). Thirdly, in the double transgenic
 331 plants BZR1R/miROE8, the leaf angle was increased compared with BZR1R (Fig. 6F;
 332 S4), which further confirmed that *OsMIR396d* was possibly epistatic to *OsBZR1*.
 333 Finally, the miROE8 seedlings with a decreased *OsGRF4* transcript level (Liu et al.,
 334 2014) were sensitive to BR (Fig. 5). In addition, near-isogenic line carrying GL2
 335 (NIL-GL2) plants, which possessed enhanced *OsGRF4* expression, showed impaired
 336 sensitivity to BR in lamina joints (Che et al., 2015). Therefore, OsmiR396d, under the
 337 regulation of OsBZR1, may control rice leaf angle by regulating the expression of
 338 *OsGRF4*.

339 Our data support *OsMIR396d* is directly controlled by *OsBZR1* on the transcription

340 level, but we also noticed that over-expression of *OsMIR396d* in OsBZR1 RNAi
341 background only partially rescue the phenotype of OsBZR1i plant. There are three
342 potential reasons for this phenomenon. Firstly, OsBZR1 is not only involved in BR
343 signaling, but also participates in some other biological processes. There are
344 thousands of target genes of OsBZR1, such as *OsLIC*, *DLT*, *IBH1*, *IL11* and so on
345 (Tong & Chu, 2009; Zhang *et al.*, 2009; Sun *et al.*, 2010; Zhang *et al.*, 2012).
346 *OsMIR396d* is just one of its targets, so *OsMIR396d* alone is not enough to explain all
347 phenotypes of OsBZR1i plant, even the phenotypes specific to BR response.
348 Secondly, *OsMIR396d* is not only controlled by OsBZR1 but also controlled by other
349 transcription factors, such as unknown GA response factors mentioned below.
350 Thirdly, there are twelve putative targets (*OsGRFs*) of OsmiR396d, and they are
351 involved in different development progress. Some of them are not involved in
352 OsBZR1 regulated signaling pathway. For example, OsGRF3 and OsGRF10 regulate
353 meristem function through repressing the expression of KNOX gene *OsKN2* (Kuijt *et*
354 *al.*, 2014), OsGRF6 is involved in IAA regulation to control panicle size (Gao *et al.*,
355 2015), OsGRF6 and OsGRF10 also influence flower organ development through
356 binding to the promoters of *OsJMJ706* and *OsCR4* (Liu *et al.*, 2014). So OsBZR1 and
357 OsmiR396d are not in a single signaling pathway, but in a complex network system,
358 their function just partially overlay with each other. In this study, we only reveal one
359 kind of connections between OsBZR1 and OsmiR396d through biochemical and
360 genetic approaches.

361 **OsmiR396d regulates *OsGRF6* to control rice plant height through GA pathway**

362 The plant height of BZR1R/miROE8 and miROE8/*d61* were shorter than both parent
363 plants (Fig. 6F, S4). The additive genetic effect between *OsMIR396d* and these BR
364 signaling pathway genes may result from the fact that OsmiR396d and its target genes
365 are not only involved in BR signaling but also in other hormone responses. Our
366 experiments showed that over-expression of *OsMIR396d* caused enhanced BR signal
367 and reduced GA signal in rice seedlings (Fig. 5, 7). In the *osgrf6* mutant, the BR
368 sensitivity was similar to wild type (Fig. 8), however, both GA signaling and
369 biosynthesis were impaired (Fig. 9). Furthermore, the expression of both *OsMIR396d*

370 and *OsGRF6* were regulated by GA. *OsMIR396d* expression level was downregulated
371 by treatment with GA biosynthesis inhibitor PAC, but was upregulated by treatment
372 with high concentrations of GA. However, the *OsGRF6* transcript level was changed in
373 an opposite way to *OsMIR396d* (Supplemental Fig. S5). These results indicate that
374 *OsmiR396d* controls rice height by directly regulating *OsGRF6* expression and GA
375 signaling.

376 ***OsmiR396d* integrates different hormone regulation pathway**

377 Our results showed that *OsMIR396d* transcription was induced by both exogenous
378 BR and GA, and *OsMIR396d* can be directly activated by OsBZR1. Based on a
379 previous report that the protein level of OsBZR1 decreased under 10^{-5} M GA₃ treatment
380 (Tong et al., 2014), the transcription level of OsBZR1's target gene *OsMIR396d* should
381 decrease under the same GA₃ concentration. However, qRT-PCR results showed that
382 the transcripts of *OsMIR396d* were increased (Supplemental Fig. S5). These conflicting
383 results implied that there might be another GA response factor, but not OsBZR1, which
384 also controlled the transcription of *OsMIR396d* in GA signal. As one of *OsmiR396d*
385 targets, *OsGRF4* functions in the BR response but not in GA signaling to control seed
386 size and leaf angle (Che et al., 2015; Duan et al., 2015). Here, we reported another
387 target of *OsmiR396d*, *OsGRF6*, was involved in GA biosynthesis regulation and signal
388 transduction to regulate plant height, but did not directly participate in the BR response
389 to control leaf angle. In addition, *OsmiR396d*-*OsGRF6* was also involved in auxin
390 signaling to determine panicle architecture (Gao et al., 2015). Therefore, *OsMIR396d*
391 could be regulated by BR, GA and auxin respectively, and controls various yield traits
392 through different downstream targets.

393 ***OsmiR396d* positively regulates BR signaling but negatively regulates GA** 394 **function**

395 Although BR and GA coordinately regulate plant development, they are distinct
396 from each other in the specific biological processes. GA powerfully promotes cell
397 elongation in a great range of concentrations, while BR only moderately promotes cell
398 elongation under specific physiological concentrations (Tong *et al.*, 2014). BR is a
399 master controller of leaf angle, while GA has only limited effect on this aspect (Tong

400 & Chu, 2016). Here, we report that OsmiR396d positively regulate BR signaling
401 mainly focused on leaf angle, and OsmiR396d negatively control GA biosynthesis
402 and signaling mainly focused on plant height. Furtherly, we found that *OsMIR396d*
403 expression is also differentially regulated by different concentrations of GA. The
404 expression of *OsMIR396d* is downregulated by low GA conditions, while upregulated
405 by high GA conditions (Supplemental Fig. S5). It indicated that the repression of GA
406 biosynthesis by OsmiR396d is attenuated when GA signaling is weak, and is
407 enhanced when GA signaling is strong. It hints OsmiR396d possibly participate in the
408 feedback regulation of GA biosynthesis. In addition, *OsMIR396d* expression is
409 upregulated under exogenous 1 μ M BR treatment (Fig. 5C). It suggested that the
410 repression of GA biosynthesis by OsmiR396d will become stronger when BR
411 signaling is greatly enhanced.

412 **Improving agronomic traits through manipulating miR396-GRF regulated** 413 **pathways**

414 Rice miR396 family and their targets control various yield traits via multiple
415 phytohormone signals. OsmiR396-OsGRF6 controls plant height and panicle size
416 (Gao *et al.*, 2015), while OsmiR396-OsGRF4 controls leaf angle and seed size (Che *et*
417 *al.*, 2015; Duan *et al.*, 2015). So it's possible to improve these traits at the same time
418 through regulating the expression of multiple OsmiR396 family members or their
419 targets. Enhancing the expression of *OsGRF4* and *OsGRF6* directly may cause more
420 spikelet, increased seed size, erect leaves and slightly higher plant height, which may
421 be close to the concept of ideal plant architecture for high grain yield breeding. Now,
422 it is also possible to create OsmiR396d resistant *OsGRF4* and *OsGRF6* alleles
423 through CRISPR-Cas9 nickase-cytidine deaminase fusion system (Zong *et al.*, 2017)
424 to convert C to T in OsmiR396 targeted DNA regions. Additional approach may also
425 be achieved through combining different members of OsmiR396 deleted
426 "non-transgenic" mutants by CRISPR-CAS9 technology (Feng *et al.*, 2013) to
427 improve rice yield.

428 In this study, an important component of the BR signaling, OsBZR1, was identified
429 as the first direct upstream regulator of *OsMIR396d*. OsmiR396d can integrate the BR

430 and GA signal interaction network to control rice plant architecture by repressing the
431 expression of multiple target genes, such as *OsGRF4* and *OsGRF6*, which participate in
432 BR and GA regulation, respectively (Fig. 10). Effective regulation of the expression of
433 *OsMIR396* and its target genes may not only increase spikelet number (Gao et al.,
434 2015) and seed size (Che et al., 2015; Duan et al., 2015), but also improve plant
435 architecture.

436 MATERIALS AND METHODS

437 Plant materials and growth conditions

438 Rice (*Oryza sativa*) Japonica cultivars Zhonghua 10 (ZH10), Nipponbare (NIP), and
439 Dongjin (DJ) were used in this study. Transgenic plants were produced in our
440 laboratory, including: *OsMIR396d* over-expression lines (miROE); *OsGRF6* antisense
441 plants (GRF6as); the *OsmiR396d*-resistant form of *OsGRF6* transgenic plants
442 (rGRF6OE); *OsLIC* antisense plants (LIC-AS); *OsBZR1* over-expression plants
443 (BZR1-OE); and *OsBZR1* RNAi interference plants (BZR1R) (Bai et al., 2007; Zhang
444 et al., 2012; Liu et al., 2014). The T3 generation of double transgenic plants
445 BZR1R/miROE8 and the F3 generation of cross progenies miROE8/*d61* were used in
446 this study. The *osgrf6* mutant from the Dongjin background was obtained from the Rice
447 Functional Genomics Express Database of Korea (Jeong et al., 2002). Mutant *d61* was
448 kindly provided by Makoto Matsuoka (Yamamuro et al., 2000). Rice plants used in this
449 study were grown in a greenhouse at 30°C/25°C (day/night) or in the field located in
450 Beijing under natural conditions.

451 Hormone treatment

452 For BR treatment, rice seeds were sterilized with 5% NaClO₃ and grown in 1/2
453 Murashige and Skoog (MS) medium (M519, Phytotech, China) with different
454 concentrations of 24-epibrassinolide (24-eBL) (CE5051, Coolaber, China) for one
455 week and the seminal root length was measured. The lamina inclination experiment
456 was carried out according to Zhang et al. (2012).

457 To detect GA sensitivity, rice seeds were first soaked in 10⁻⁵ M paclobutrazol (PAC)

458 (CP8121, Coolaber, China) for 2 days to inhibit endogenous GA biosynthesis, and then
459 germinated seeds were planted in Yoshida's culture solution (Yoshida et al., 1976) with
460 various concentrations of GA₃ (G8040, Solarbio, China). After 10 days of growth, the
461 length of the second leaf sheath was measured, and the seedlings were used to detect the
462 transcription levels of *OsMIR396d* and *OsGRF6*.

463 **Microscopy observation**

464 For scanning electron microscopy (SEM) analysis, the lamina joints of *OsMIR396d*
465 over-expression plants and wild type ZH10 at heading stage were excised to image the
466 adaxial surface according to Wang et al. (2008). To determine the cell length of second
467 leaf sheaths, surface cells in the same position of the second leaf sheaths of miROE,
468 *osgrf6*, and wild type ZH10 and DJ 2-week-old seedlings were torn off and observed
469 under Differential Interference Contrast (DIC) microscopy according to Li et al (2011).

470 **Flow cytometric analysis of cell cycle progression**

471 For flow cytometry, wild type and miROE seeds were germinated for 7 days in petri
472 dishes (diameter, 20 cm) on filter paper with sterilized water in the dark at 28°C. Root
473 apical tips (1 mm) were excised and immediately collected in chilled chopping buffer,
474 and chopped with a single-edged razor blade in a glass petri dish (diameter, 5 cm) on
475 ice. Chopping buffer (45 mM MgCl₂, 30 mM sodium citrate, 20 mM
476 4-morpholinepropane sulfonate, and 1 mg ml⁻¹ triton X-100, pH 7.0) was used to
477 release cells from the chopped tissues. The DNA content of individual cells was
478 determined by flow cytometry. Cell nuclei were prepared for FACS Aria™ by staining
479 with 2 µg ml⁻¹ 4',6-diamidino-2-phenylindole (DAPI). Each Root apical tip sample was
480 prepared three times and subjected to FACS Caliber cytometry (BD Bioscience, USA)
481 three times. Ten thousand nuclei were measured per analysis as previously described
482 (Ma et al., 2009).

483 **RNA extraction and qRT-PCR**

484 Total RNA was extracted from 2-week-old rice seedlings using the Trizol RNA
485 extraction kit according to the user manual (15596, Invitrogen, USA). First-strand

486 cDNA was then synthesized from 1-2 µg total RNA using the FastQuant RT Kit (with
487 gDNase) (KR106, Tiangen, China) according to the manufacturer's instructions.
488 qRT-PCR analyses were carried out using the SYBR Green Master Mix (QPK-201,
489 TOYOBO, Japan) on the Mx3000P real-time PCR System (Stratagene, USA)
490 according to the manufacturer's instructions. Rice *UBIQUITIN* was used as internal
491 reference, and gene expression levels were normalized to the expression level of
492 *UBIQUITIN*. The expression level of *OsMIR396d* was analyzed as described by Liu et
493 al. (2014). All primers are described in Table S1.

494 **ChIP-qPCR**

495 Two grams of leaves from 2-week-old rice seedlings of wild type (ZH10) and
496 *OsBZR1* RNAi plants (BZR1R) were used for chromatin immunoprecipitation (ChIP)
497 assay; the experiment was performed as described in He et al. (2005). The OsBZR1
498 antibody was used for immunoblot and ChIP analysis. The immunoprecipitated DNA
499 content was determined by qPCR. Three replications were performed independently.
500 The primers used in ChIP assays are listed in Table S1.

501 **Yeast one-hybrid assays**

502 Yeast one-hybrid assays were used to check binding of OsBZR1 to the *OsMIR396d*
503 promoter according to a previous study (Chen et al., 2013). The wild-type putative
504 OsBZR1 binding sites, S1, S2, S3 and mutated site S1 (mS1) of the *OsMIR396d*
505 promoter tandem repeat sequences (S1, CGTCGTGTGGAA; S2, GTTCGTGCGTCT;
506 S3, CGGCGTGTGTGT; and mS1, CGTAAAAAAGAA) were placed upstream of the
507 minimal promoter in pHISi-1 vector. The full-length coding region of *OsBZR1* was
508 fused to the pGAD424 vector. pGAD424-*OsBZR1* was then transformed into the yeast
509 strain YM4271, which carries the reporter gene *HIS3* under the control of wild-type
510 S1/S2/S3 or mS1. The transformed yeast cells were selected on SD/-His/-Leu medium
511 containing 0, 15, 30, 45 and 60 mM 3-AT (a competitive inhibitor of the *HIS3* gene
512 product) by standard protocols (Clontech, USA) and 15 mM 3-AT was used as the final
513 concentration for screening.

514 **EMSA**

515 The full-length cDNA of *OsBZR1* was fused into the *KpnI* and *EcoRI* sites of vector
516 pCold™ TF DNA. The fusion protein was purified with Ni Sepharose High
517 Performance purification column (17-5268, Amersham, Sweden) according to the
518 product manual. Biotin end-labeled DNA fragment of the *OsMIR396d* promoter was
519 prepared by PCR amplification using 5'-biotin labeled primers,
520 5'-CGGGATCGTGCAATTCTCA-3' and 5'-TAAATAGCGGGAGGAGATAACC-3'.
521 EMSA assay was performed using the LightShift Chemiluminescent EMSA Kit
522 (20148, Thermo, USA) according to the manufacturer's instructions. Briefly, the
523 reaction mixtures (20 µL) for EMSA contained 2 µg purified OsBZR1, 20 fmol biotin
524 end-labeled target DNA, 2 µL 10× Binding Buffer, 1 µL 1µg µL⁻¹ Poly (dI•dC) and
525 double-distilled water. The binding reactions were incubated at room temperature for
526 20 min and electrophoresed on a 10% native polyacrylamide gel, then transferred to a
527 nylon membrane (S4056, Millipore, USA) in 0.5× TBE buffer at 380 mA for 60 min.
528 Biotin-labeled DNA was detected by chemiluminescence.

529 **Transient assays for activation activity *in vivo***

530 The transcriptional activity assay was carried out in the transient-transformed
531 protoplast prepared from 4-week-old *Arabidopsis* seedlings of the Columbia line
532 grown in short day conditions as described previously (Lin et al., 2007). For the specific
533 binding and activating activity of OsBZR1 to the *OsMIR396d* promoter assay,
534 full-length cDNA of *OsBZR1* were fused into the pBI221-GFP vector driven by the
535 CaMV 35S promoter to generate pBI221-OsBZR1-GFP. The pBI221-GFP vector was
536 used as the negative control. The *OsMIR396d* promoter was amplified to generate the
537 *OsMIR396d::LUC* reporter gene. The plasmid carrying the *GUS* gene under the control
538 of the CaMV 35S promoter was used as a normalization control. Values represent
539 means ± SD of three technical replicates.

540 **GA quantification**

541 For GA quantification of Dongjin and *osgrf6* plants, 3 grams of 2-week-old seedlings
542 were harvested and frozen in liquid nitrogen. Quantification of endogenous GAs was
543 performed as described previously (Li et al., 2011).

544 **SUPPLEMENTAL DATA**

545 **Supplemental Figure S1.** The expression level of several BR related genes in
546 miROEs.

547 **Supplemental Figure S2** The expression pattern of *OsGRFs* under 24-eBL treatment.

548 **Supplemental Figure S3** The expression of *OsBZR1* in miROE8 and BZR1R/miROE
549 double transgenic lines.

550 **Supplemental Figure S4** Genetic relationship of *OsMIR396d* and *OsBZR1* or *D61*.

551 **Supplemental Figure S5** The expression pattern of *OsMIR396d* and *OsGRF6* under
552 PAC or GA₃ treatment.

553 **Supplemental Figure S6** The sensitivity of *osgrf6* to GA was decreased compared
554 with DJ.

555 **Supplemental Table S1.** List of primers used in this study.

556 **ACKNOWLEDGEMENTS**

557 We would like to thank Dr J. H. Snyder for examining the English usage in the
558 manuscript, Wuhan Greensword Creation Technology Co., Ltd. for Gibberellin
559 measurements, and Yuda Niu for rice transformation.

560 **FIGURE LEGENDS**

561 **Figure 1.** The leaf angle of *OsMIR396d* over-expression plants was increased.

562 A. The third leaf angle of miROEs was specifically increased. Bar = 1 cm.

563 B. Statistical analysis of leaf angles. The third leaf angle was measured at the seedling
564 stage and the angles of the top three leaves were measured at the seed filling stage.

565 Error bars indicate SD for at least fifteen plants. Asterisks indicate $P < 0.01$ (**)
566 compared with wild type in the Student's t test analysis.

567 **Figure 2.** The plant height and length of internodes in *OsMIR396d* over-expression
568 plants were reduced.

569 A. The phenotype of miROEs and ZH10 at the seed filling stage. Bar = 5 cm.

570 B. The panicle and internodes of miROEs and ZH10. Bar = 5 cm.

571 C. Results of statistical analysis of plant height and internode length of miROE lines
572 and ZH10. More than fifteen mature plants were used in each analysis.

573 D. Results of statistical analysis of fifth internode lengths of miROEs and ZH10. Error
574 bars indicate SD for at least fifteen plants. Asterisks indicate $P < 0.01$ (**)
575 compared with ZH10 in the Student's t test analysis.

576 E. Relative internode length of miROEs and ZH10. The data shows each internode
577 length relative to the total culm length. Error bars indicate SD for at least fifteen plants.
578 Asterisks indicate $P < 0.05$ (*) and $P < 0.01$ (**)
579 compared with ZH10 in the Student's t test analysis.

580 **Figure 3.** Scanning electron microscopic examination of the leaf lamina joint.

581 A, B. Adaxial surface of the leaf lamina joint in ZH10 (A) and miROE8 (B). Arrows
582 indicate the increased growth of cells.

583 C, D. Longitudinal sections of the leaf lamina joint of ZH10 (C) and miROE8 (D). Half
584 frame indicated regions were used to calculate cell layers.

585 E, F. Close-up of regions denoted by rectangles in (C) and (D) respectively. Ad,
586 adaxial; Ab, abaxial. Scale bars = 200 μm .

587 G. Statistical analysis of cell length in (C) and (F). Cell length along the adaxial-abaxial
588 axis and proximal-distal axis were measured respectively. Error bars indicate SD for at
589 least 100 cells. Asterisks indicate $P < 0.01$ (**)
589 compared with ZH10 in the Student's t

590 test analysis.

591 **Figure 4.** Cell length and cell division analysis.

592 A. The second leaf sheath cells of 2-week-old seedlings of miROE8 and ZH10. Bars =
593 50 μm .

594 B. The statistical analysis of cell length in the second leaf sheath. Error bars indicate SD
595 for more than 400 cells. Asterisks indicate $P < 0.01$ (**) compared with ZH10 in
596 student's t test analysis.

597 C. The DNA content of miROE8 and ZH10. After the seeds germinated for 3 days at
598 28°C , the root tips were harvested. Cell nuclei (10,000) were stained with $1 \mu\text{g mL}^{-1}$
599 DAPI and analyzed by flow cytometry. 2C and 4C represent the DAPI signals that
600 correspond to nuclei with different DNA contents.

601 D. Cell mitotic index in root apical meristem in miROE8 and ZH10. The results were
602 from three independent replications. Error bars indicate SD. Asterisks indicate $P < 0.01$
603 (**) compared with ZH10 in the Student's t test analysis.

604 **Figure 5.** OsmiR396d is involved in BR signaling.

605 A. Lamina joint inclination assay of miROE8 and ZH10. The second lamina joints of
606 one-week-old seedlings grown under dark condition were cut off and treated with
607 different concentrations of 24-eBL for three days. Error bars indicate SD for at least
608 fifteen plants. Asterisks indicate $P < 0.05$ (*) and $P < 0.01$ (**) compared with ZH10 in
609 the Student's t test analysis.

610 B. The seminal root growth of miROE8 and ZH10 under treatment with different
611 concentrations of 24-eBL. The seminal root length was measured after seedlings were
612 grown in 24-eBL containing 1/2 MS medium for one week. Error bars indicate SD for
613 at least fifteen plants. Asterisks indicate $P < 0.05$ (*) and $P < 0.01$ (**) compared with
614 ZH10 in the Student's t test analysis.

615 C. The expression pattern of *OsMIR396d* under treatment with 24-eBL. Two-week-old
616 ZH10 seedlings were treated with $1 \mu\text{M}$ 24-eBL. Whole plants were sampled 1, 3, 6, 12
617 and 24 h after treatment. The plants sampled from the normal growth condition were
618 used as control. *UBQUITINI* was used as a reference gene. Error bars indicate SD for
619 three replicates. Asterisks indicate $P < 0.05$ (*) and $P < 0.01$ (**) compared with control

620 in the Student's t test analysis.
621 D. The expression of *OsMIR396d* in *OsLIC* antisense plants (LIC-AS), *OsBZR1* RNAi
622 plants (BZR1R), and *OsBZR1* over-expression (BZR1-OE) plants. LIC-AS and
623 BZR1R were under the background of ZH10 and BZR1-OE was under the background
624 of Nipponbare (NIP). *UBQUITINI* was used as reference gene. Error bars indicate SD
625 for three replicates. Asterisks indicate $P < 0.05$ (*) and $P < 0.01$ (**) compared with
626 wild-type ZH10 or NIP respectively in the Student's t test analysis.

627 **Figure 6.** *OsBZR1* directly activates the expression of *OsMIR396d*.

628 A. Localization of three putative *OsBZR1* binding sites S1, S2, and S3 in the
629 *OsMIR396d* promoter.

630 B. Yeast one-hybrid analysis of *OsBZR1* binding the promoter of *OsMIR396d*. Empty
631 pHIS vector was used as negative control.

632 C. EMSA analysis of *OsBZR1* binding the promoter of *OsMIR396d*. S1-containing
633 DNA fragment was labeled with biotin. The arrow indicates the complex of
634 *OsBZR1*-His and the DNA probe.

635 D. ChIP-qPCR analysis of *OsBZR1* binding the promoter of *OsMIR396d* using
636 *OsBZR1* antibody to enrich DNA. The *UBIQUITIN* DNA fragment was used as an
637 internal control. Error bars indicate SD for three replicates. Asterisks indicate $P < 0.01$
638 (**) compared with ZH10 in the Student's t test analysis.

639 E. Transactivation assay of *OsBZR1* with the luciferase reporter system. Error bars
640 indicate SD for three replicates. Asterisks indicate $P < 0.01$ (**) compared with control
641 in the Student's t test analysis.

642 F. The phenotype of *OsBZR1* RNA interference transgenic plants (*miROE8/BZR1R*)
643 under the background of *miROE8*. Bar = 10 cm.

644 **Figure 7.** GA signaling and biosynthesis were impaired in *OsMIR396d*
645 over-expression plants.

646 A. The phenotype of *miROE8* and ZH10 seedlings growth under different
647 concentrations of GA_3 treatment. The seeds were treated with 10 μ M PAC for 2 days
648 before cultivation in nutrient solution containing the indicated concentration of GA_3 .
649 After 10 days of growth, the seedlings were photographed. The measurements of the

650 second leaf sheath are shown. Error bars indicate SD for at least fifteen plants. Bar = 5
651 cm.

652 B. The expression of GA pathway related genes in miROE and ZH10. *UBQUITINI* was
653 used as reference gene. Error bars indicate SD for three replicates.

654 **Figure 8.** BR signaling was not affected in *osgrf6* mutant.

655 A. The phenotype of *OsGRF6* antisense transgenic plant (GRF6as) and the
656 OsmiR396d-resistant form of *OsGRF6* transgenic plant (rGRF6OE). Bar = 5 cm.

657 B. The second leaf sheath cells of 2-week-old seedlings of *osgrf6* and DJ. The cell
658 length was measured. Error bars indicate SD for more than 400 cells. Asterisks indicate
659 $P < 0.01$ (**) compared with DJ in the Student's t test analysis. Bar = 50 μm .

660 C. The leaf angle of *osgrf6* was not changed. The third leaf angle was measured. Error
661 bars indicate SD for at least fifteen plants.

662 D. Lamina joint inclination assay of *osgrf6* and DJ. Error bars indicate SD for at least
663 fifteen plants.

664 E. The seminal root growth of miROE8 and ZH10 under treatment with different
665 concentrations of 24-eBL. Error bars indicate SD for at least fifteen plants.

666 **Figure 9.** GA signaling and biosynthesis are impaired in the *osgrf6* mutant.

667 A. *osgrf6* and DJ seedlings treated with PAC or GA_3 . The seeds were treated with water
668 (control) or 10^{-5} M PAC for 2 days, and then germinated seeds were planted in PAC
669 and/or GA_3 containing culture solution for 10 days. Bar = 5 cm.

670 B. The statistical result of the second leaf sheath length of *osgrf6* and DJ grown under
671 PAC and/or GA_3 treatment. Error bars indicate SD for at least fifteen plants. The
672 relative leaf sheath length between DJ and *osgrf6* was calculated and shown. Asterisks
673 indicate $P < 0.01$ (**) compared with DJ in student's t test analysis.

674 C. The expression of GA pathway related genes in *osgrf6* and DJ. *UBQUITINI* was
675 used as reference gene. Error bars indicate SD for three replicates.

676 D. Quantification of endogenous GAs in *osgrf6* and DJ. Two-week-old seedlings were
677 sampled. Error bars indicate SD for three replicates. Asterisks indicate $P < 0.01$ (**)
678 compared with DJ in the Student's t test analysis.

679 **Figure 10.** A proposed model for OsmiR396d controlling rice plant architecture.

680 *OsMIR396d* is activated by OsBZR1, which is the key regulator transcription factor of
681 BR signaling. On the one hand, OsmiR396d regulates leaf angle by repressing the
682 expression of *OsGRF4*. On the other hand, OsmiR396d is involved in GA signaling and
683 biosynthesis by regulating the expression of *OsGRF6* to control rice plant height.

Parsed Citations

Ashikari M, Wu J, Yano M, Sasaki T, Yoshimura A 1999. Rice gibberellin-insensitive dwarf mutant gene Dwarf 1 encodes the α -subunit of GTP-binding protein. *Proceedings of the National Academy of Sciences* 96: 10284-10289.

Pubmed: [Author and Title](#)

CrossRef: [Author and Title](#)

Google Scholar: [Author Only](#) [Title Only](#) [Author and Title](#)

Bai MY, Shang JX, Oh E, Fan M, Bai Y, Zentella R, Sun TP, Wang ZY. 2012. Brassinosteroid, gibberellin and phytochrome impinge on a common transcription module in Arabidopsis. *Nature Cell Biology* 14: 810-817.

Pubmed: [Author and Title](#)

CrossRef: [Author and Title](#)

Google Scholar: [Author Only](#) [Title Only](#) [Author and Title](#)

Bai MY, Zhang LY, Gampala SS, Zhu SW, Song WY, Chong K, Wang ZY. 2007. Functions of OsBZR1 and 14-3-3 proteins in brassinosteroid signaling in rice. *Proceedings of the National Academy of Sciences of the United States of America* 104: 13839-13844.

Pubmed: [Author and Title](#)

CrossRef: [Author and Title](#)

Google Scholar: [Author Only](#) [Title Only](#) [Author and Title](#)

Cao HP, Chen SK. 1995. Brassinosteroid-induced rice lamina joint inclination and its relation to indole-3-acetic acid and ethylene. *Plant Growth Regulation* 16: 189-196.

Pubmed: [Author and Title](#)

CrossRef: [Author and Title](#)

Google Scholar: [Author Only](#) [Title Only](#) [Author and Title](#)

Che R, Tong H, Shi B, Liu Y, Fang S, Liu D, Xiao Y, Hu B, Liu L, Wang H, et al. 2015. Control of grain size and rice yield by GL2-mediated brassinosteroid responses. *Nature Plants* 2: 15195.

Pubmed: [Author and Title](#)

CrossRef: [Author and Title](#)

Google Scholar: [Author Only](#) [Title Only](#) [Author and Title](#)

Chen Y, Li F, Ma Y, Chong K, Xu Y. 2013. Overexpression of OrbHLH001, a putative helix-loop-helix transcription factor, causes increased expression of AKT1 and maintains ionic balance under salt stress in rice. *J Plant Physiol* 170: 93-100.

Pubmed: [Author and Title](#)

CrossRef: [Author and Title](#)

Google Scholar: [Author Only](#) [Title Only](#) [Author and Title](#)

Clouse SD, Langford M, McMorris TC. 1996. A brassinosteroid-insensitive mutant in Arabidopsis thaliana exhibits multiple defects in growth and development. *Plant Physiology* 111: 671-678.

Pubmed: [Author and Title](#)

CrossRef: [Author and Title](#)

Google Scholar: [Author Only](#) [Title Only](#) [Author and Title](#)

Duan P, Ni S, Wang J, Zhang B, Xu R, Wang Y, Chen H, Zhu X, Li Y. 2015. Regulation of OsGRF4 by OsmiR396 controls grain size and yield in rice. *Nature Plants* 2: 15203.

Pubmed: [Author and Title](#)

CrossRef: [Author and Title](#)

Google Scholar: [Author Only](#) [Title Only](#) [Author and Title](#)

Fan LM, Feng X, Wang Y, Deng XW. 2007. Gibberellin signal transduction in rice. *Journal of Integrative Plant Biology* 49: 731-741.

Pubmed: [Author and Title](#)

CrossRef: [Author and Title](#)

Google Scholar: [Author Only](#) [Title Only](#) [Author and Title](#)

Fariduddin Q, Yusuf M, Ahmad I, Ahmad A 2014. Brassinosteroids and their role in response of plants to abiotic stresses. *Biologia Plantarum* 58: 9-17.

Pubmed: [Author and Title](#)

CrossRef: [Author and Title](#)

Google Scholar: [Author Only](#) [Title Only](#) [Author and Title](#)

Feng Z, Zhang B, Ding W, Liu X, Yang DL, Wei P, Cao F, Zhu S, Zhang F, Mao Y, et al. 2013. Efficient genome editing in plants using a CRISPR/Cas system. *Cell Res* 23: 1229-1232.

Pubmed: [Author and Title](#)

CrossRef: [Author and Title](#)

Google Scholar: [Author Only](#) [Title Only](#) [Author and Title](#)

Gallego-Bartolome J, Minguet EG, Grau-Enguix F, Abbas M, Locascio A, Thomas SG, Alabadi D, Blazquez MA. 2012. Molecular mechanism for the interaction between gibberellin and brassinosteroid signaling pathways in Arabidopsis. *Proceedings of the National Academy of Sciences of the United States of America* 109: 13446-13451.

Pubmed: [Author and Title](#)

CrossRef: [Author and Title](#)

Google Scholar: [Author Only](#) [Title Only](#) [Author and Title](#)

Gao F, Wang K, Liu Y, Chen Y, Chen P, Shi Z, Luo J, Jiang D, Fan F, Zhu Y, et al. 2015. Blocking miR396 increases rice yield by shaping inflorescence architecture. *Nature Plants* 2: 15196.

Pubmed: [Author and Title](#)

CrossRef: [Author and Title](#)

Google Scholar: [Author Only](#) [Title Only](#) [Author and Title](#)

Greenboim-Wainberg Y, Maymon I, Borochoy R, Alvarez J, Olszewski N, Ori N, Eshed Y, Weiss D. 2005. Cross talk between gibberellin and cytokinin: The *Arabidopsis* GA response inhibitor SPINDLY plays a positive role in cytokinin signaling. *Plant Cell* 17: 92-102.

Pubmed: [Author and Title](#)

CrossRef: [Author and Title](#)

Google Scholar: [Author Only](#) [Title Only](#) [Author and Title](#)

Hao Z, Gui-Lu TAN, Ya-Guang XUE, Zhi-Qin W, Li-Jun LIU, Jian-Chang Y. 2010. Changes in grain yield and morphological and physiological characteristics during 60-year evolution of japonica rice Cultivars in Jiangsu Province, China. *Acta Agronomica Sinica* 36: 133-140.

Pubmed: [Author and Title](#)

CrossRef: [Author and Title](#)

Google Scholar: [Author Only](#) [Title Only](#) [Author and Title](#)

He JX, Gendron JM, Sun Y, Gampala SSL, Gendron N, Sun CQ, Wang ZY. 2005. BZR1 is a transcriptional repressor with dual roles in brassinosteroid homeostasis and growth responses. *Science* 307: 1634-1638.

Pubmed: [Author and Title](#)

CrossRef: [Author and Title](#)

Google Scholar: [Author Only](#) [Title Only](#) [Author and Title](#)

Hedden P, Sponsel V. 2015. A century of gibberellin research. *Journal of Plant Growth Regulation* 34: 740-760.

Pubmed: [Author and Title](#)

CrossRef: [Author and Title](#)

Google Scholar: [Author Only](#) [Title Only](#) [Author and Title](#)

Hirano K, Asano K, Tsuji H, Kawamura M, Mori H, Kitano H, Ueguchi-Tanaka M, Matsuoka M. 2010. Characterization of the molecular mechanism underlying gibberellin perception complex formation in rice. *Plant Cell* 22: 2680-2696.

Pubmed: [Author and Title](#)

CrossRef: [Author and Title](#)

Google Scholar: [Author Only](#) [Title Only](#) [Author and Title](#)

International Rice Genome Sequencing P. 2005. The map-based sequence of the rice genome. *Nature* 436: 793-800.

Pubmed: [Author and Title](#)

CrossRef: [Author and Title](#)

Google Scholar: [Author Only](#) [Title Only](#) [Author and Title](#)

Itoh H, Tatsumi T, Sakamoto T, Otomo K, Toyomasu T, Kitano H, Ashikari M, Ichihara S, Matsuoka M. 2004. A rice semi-dwarf gene, *Tan-Ginbozu* (D35), encodes the gibberellin biosynthesis enzyme, ent-kaurene oxidase. *Plant Molecular Biology* 54: 533-547.

Pubmed: [Author and Title](#)

CrossRef: [Author and Title](#)

Google Scholar: [Author Only](#) [Title Only](#) [Author and Title](#)

Jeong DH, An S, Kang HG, Moon S, Han JJ, Park S, Lee HS, An K, An G. 2002. T-DNA insertional mutagenesis for activation tagging in rice. *Plant Physiology* 130: 1636-1644.

Pubmed: [Author and Title](#)

CrossRef: [Author and Title](#)

Google Scholar: [Author Only](#) [Title Only](#) [Author and Title](#)

Jones-Rhoades MW, Bartel DP, Bartel B. 2006. MicroRNAs and their regulatory roles in plants. *Annual Review of Plant Biology* 57: 19-53.

Pubmed: [Author and Title](#)

CrossRef: [Author and Title](#)

Google Scholar: [Author Only](#) [Title Only](#) [Author and Title](#)

Jones-Rhoades MW, Bartel DP. 2004. Computational identification of plant MicroRNAs and their targets, including a stress-induced miRNA. *Molecular Cell* 14: 787-799.

Pubmed: [Author and Title](#)

CrossRef: [Author and Title](#)

Google Scholar: [Author Only](#) [Title Only](#) [Author and Title](#)

Khush GS. 2013. Strategies for increasing the yield potential of cereals: case of rice as an example. *Plant Breeding* 132: 433-436.

Pubmed: [Author and Title](#)

CrossRef: [Author and Title](#)

Google Scholar: [Author Only](#) [Title Only](#) [Author and Title](#)

Kim JH, Lee BH. 2006. GROWTH-REGULATING FACTOR4 of *Arabidopsis thaliana* is required for development of leaves, cotyledons, and shoot apical meristem. *Journal of Plant Biology* 49: 463-468.

Pubmed: [Author and Title](#)

CrossRef: [Author and Title](#)

Google Scholar: [Author Only](#) [Title Only](#) [Author and Title](#)

Kim TW, Guan SH, Burlingame AL, Wang ZY. 2011. The CDG1 kinase mediates brassinosteroid signal transduction from BRI1 receptor kinase to BSU1 phosphatase and GSK3-like kinase BIN2. *Molecular Cell* 43: 561-571.

Pubmed: [Author and Title](#)

CrossRef: [Author and Title](#)

Google Scholar: [Author Only Title Only Author and Title](#)

Kuijt SJ, Greco R, Agalou A, Shao J, 't Hoen CC, Overnas E, Osnato M, Curiale S, Meynard D, van Gulik R, et al. 2014. Interaction between the GROWTH-REGULATING FACTOR and KNOTTED1-LIKE HOMEODOMAIN families of transcription factors. *Plant Physiology* 164: 1952-1966.

Pubmed: [Author and Title](#)

CrossRef: [Author and Title](#)

Google Scholar: [Author Only Title Only Author and Title](#)

Li J, Jiang J, Qian Q, Xu Y, Zhang C, Xiao J, Du C, Luo W, Zou G, Chen M, et al. 2011. Mutation of rice BC12/GDD1, which encodes a kinesin-like protein that binds to a GA biosynthesis gene promoter, leads to dwarfism with impaired cell elongation. *Plant Cell* 23: 628-640.

Pubmed: [Author and Title](#)

CrossRef: [Author and Title](#)

Google Scholar: [Author Only Title Only Author and Title](#)

Li J, Wen JQ, Lease KA, Doko JT, Tax FE, Walker JC. 2002. BAK1, an Arabidopsis LRR receptor-like protein kinase, interacts with BRI1 and modulates brassinosteroid signaling. *Cell* 110: 213-222.

Pubmed: [Author and Title](#)

CrossRef: [Author and Title](#)

Google Scholar: [Author Only Title Only Author and Title](#)

Li JM, Nam KH, Vafeados D, Chory J. 2001. BIN2, a new brassinosteroid-insensitive locus in Arabidopsis. *Plant Physiology* 127: 14-22.

Pubmed: [Author and Title](#)

CrossRef: [Author and Title](#)

Google Scholar: [Author Only Title Only Author and Title](#)

Li QF, Wang CM, Jiang L, Li S, Sun SSM, He JX. 2012. An interaction between BZR1 and DELLAs mediates direct signaling crosstalk between brassinosteroids and gibberellins in Arabidopsis. *Science Signaling* 5.

Pubmed: [Author and Title](#)

CrossRef: [Author and Title](#)

Google Scholar: [Author Only Title Only Author and Title](#)

Lin RC, Ding L, Casola C, Ripoll DR, Feschotte C, Wang HY. 2007. Transposase-derived transcription factors regulate light signaling in Arabidopsis. *Science* 318: 1302-1305.

Pubmed: [Author and Title](#)

CrossRef: [Author and Title](#)

Google Scholar: [Author Only Title Only Author and Title](#)

Liu D, Song Y, Chen Z, Yu D. 2009. Ectopic expression of miR396 suppresses GRF target gene expression and alters leaf growth in Arabidopsis. *Physiologia Plantarum* 136: 223-236.

Pubmed: [Author and Title](#)

CrossRef: [Author and Title](#)

Google Scholar: [Author Only Title Only Author and Title](#)

Liu H, Guo S, Xu Y, Li C, Zhang Z, Zhang D, Xu S, Zhang C, Chong K. 2014. OsmiR396d-regulated OsGRFs function in floral organogenesis in rice through binding to their targets OsJM706 and OsCR4. *Plant Physiology* 165: 160-174.

Pubmed: [Author and Title](#)

CrossRef: [Author and Title](#)

Google Scholar: [Author Only Title Only Author and Title](#)

Liu J, Chen J, Zheng X, Wu F, Lin Q, Heng Y, Tian P, Cheng Z, Yu X, Zhou K, et al. 2017. GW5 acts in the brassinosteroid signalling pathway to regulate grain width and weight in rice. *Nature Plants* 3: 17043.

Pubmed: [Author and Title](#)

CrossRef: [Author and Title](#)

Google Scholar: [Author Only Title Only Author and Title](#)

Luo AD, Liu L, Tang ZS, Bai XQ, Cao SY, Chu CC. 2005. Down-regulation of OsGRF1 gene in rice rhd1 mutant results in reduced heading date. *Journal of Integrative Plant Biology* 47: 745-752.

Pubmed: [Author and Title](#)

CrossRef: [Author and Title](#)

Google Scholar: [Author Only Title Only Author and Title](#)

Ma Q, Dai X, Xu Y, Guo J, Liu Y, Chen N, Xiao J, Zhang D, Xu Z, Zhang X, et al. 2009. Enhanced tolerance to chilling stress in OsMYB3R-2 transgenic rice is mediated by alteration in cell cycle and ectopic expression of stress genes. *Plant Physiology* 150: 244-256.

Pubmed: [Author and Title](#)

CrossRef: [Author and Title](#)

Google Scholar: [Author Only Title Only Author and Title](#)

McGinnis KM, Thomas SG, Soule JD, Strader LC, Zale JM, Sun TP, Steber CM. 2003. The Arabidopsis SLEEPY1 gene encodes a putative F-box subunit of an SCF E3 ubiquitin ligase. *Plant Cell* 15: 1120-1130.

Pubmed: [Author and Title](#)
CrossRef: [Author and Title](#)
Google Scholar: [Author Only Title Only Author and Title](#)

Mora-Garcia S, Vert G, Yin Y, Cano-Delgado A, Cheong H, Chory J. 2004. Nuclear protein phosphatases with Kelch-repeat domains modulate the response to brassinosteroids in Arabidopsis. *Genes & Development* 18: 448-460.

Pubmed: [Author and Title](#)
CrossRef: [Author and Title](#)
Google Scholar: [Author Only Title Only Author and Title](#)

Nakamura A, Fujioka S, Sunohara H, Kamiya N, Hong Z, Inukai Y, Miura K, Takatsuto S, Yoshida S, Ueguchi-Tanaka M, et al. 2006. The role of OsBRI1 and its homologous genes, OsBRL1 and OsBRL3, in rice. *Plant Physiology* 140: 580-590.

Pubmed: [Author and Title](#)
CrossRef: [Author and Title](#)
Google Scholar: [Author Only Title Only Author and Title](#)

Qiao S, Sun S, Wang L, Wu Z, Li C, Li X, Wang T, Leng L, Tian W, Lu T, et al. 2017. The RLA1/SMOS1 transcription factor functions with OsBZR1 to regulate brassinosteroid signaling and rice architecture. *Plant Cell* 29: 292-309.

Pubmed: [Author and Title](#)
CrossRef: [Author and Title](#)
Google Scholar: [Author Only Title Only Author and Title](#)

Sakamoto T, Morinaka Y, Ohnishi T, Sunohara H, Fujioka S, Ueguchi-Tanaka M, Mizutani M, Sakata K, Takatsuto S, Yoshida S, et al. 2006. Erect leaves caused by brassinosteroid deficiency increase biomass production and grain yield in rice. *Nature Biotechnology* 24: 105-109.

Pubmed: [Author and Title](#)
CrossRef: [Author and Title](#)
Google Scholar: [Author Only Title Only Author and Title](#)

Sakata T, Oda S, Tsunaga Y, Shomura H, Kawagishi-Kobayashi M, Aya K, Saeki K, Endo T, Nagano K, Kojima M, et al. 2014. Reduction of gibberellin by low temperature disrupts pollen development in rice. *Plant Physiology* 164: 2011-2019.

Pubmed: [Author and Title](#)
CrossRef: [Author and Title](#)
Google Scholar: [Author Only Title Only Author and Title](#)

Sasaki A, Itoh H, Gomi K, Ueguchi-Tanaka M, Ishiyama K, Kobayashi M, Kitano H, Ashikari M, Matsuoka M. 2003. Characterization of rice dwarf mutant, GA insensitive dwarf 2 (gid2). *Plant and Cell Physiology* 44: S186-S186.

Pubmed: [Author and Title](#)
CrossRef: [Author and Title](#)
Google Scholar: [Author Only Title Only Author and Title](#)

Shimada A, Ueguchi-Tanaka M, Sakamoto T, Fujioka S, Takatsuto S, Yoshida S, Sazuka T, Ashikari M, Matsuoka M. 2006. The rice SPINDLY gene functions as a negative regulator of gibberellin signaling by controlling the suppressive function of the DELLA protein, SLR1, and modulating brassinosteroid synthesis. *Plant Journal* 48: 390-402.

Pubmed: [Author and Title](#)
CrossRef: [Author and Title](#)
Google Scholar: [Author Only Title Only Author and Title](#)

Simpson JF, Dutt PL, Page DL. 1992. Expression of mitoses per thousand cells and cell density in breast carcinomas: A proposal. *Human Pathology* 23: 608-611.

Pubmed: [Author and Title](#)
CrossRef: [Author and Title](#)
Google Scholar: [Author Only Title Only Author and Title](#)

Sinclair TR, Sheehy JE. 1999. Erect leaves and photosynthesis in rice. *Science* 283: 1455-1455.

Pubmed: [Author and Title](#)
CrossRef: [Author and Title](#)
Google Scholar: [Author Only Title Only Author and Title](#)

Spielmeyer W, Ellis MH, Chandler PM. 2002. Semidwarf (sd-1), "green revolution" rice, contains a defective gibberellin 20-oxidase gene. *Proceedings of the National Academy of Sciences of the United States of America* 99: 9043-9048.

Pubmed: [Author and Title](#)
CrossRef: [Author and Title](#)
Google Scholar: [Author Only Title Only Author and Title](#)

Sun S, Chen D, Li X, Qiao S, Shi C, Li C, Shen H, Wang X. 2015. Brassinosteroid signaling regulates leaf erectness in oryza sativa via the control of a specific U-type cyclin and cell proliferation. *Developmental Cell* 34: 1-9.

Pubmed: [Author and Title](#)
CrossRef: [Author and Title](#)
Google Scholar: [Author Only Title Only Author and Title](#)

Sun Y, Fan XY, Cao DM, Tang W, He K, Zhu JY, He JX, Bai MY, Zhu S, Oh E, et al. 2010. Integration of brassinosteroid signal transduction with the transcription network for plant growth regulation in Arabidopsis. *Developmental Cell* 19: 765-777.

Pubmed: [Author and Title](#)
CrossRef: [Author and Title](#)
Google Scholar: [Author Only Title Only Author and Title](#)

Tanaka A, Nakagawa H, Tomita C, Shimatani Z, Ohtake M, Nomura T, Jiang C-J, Dubouzet JG, Kikuchi S, Sekimoto H, et al. 2009. **BRASSINOSTEROID UPREGULATED1**, encoding a helix-loop-helix protein, is a novel gene involved in brassinosteroid signaling and controls bending of the lamina joint in rice. *Plant Physiology* 151: 669-680.

Pubmed: [Author and Title](#)

CrossRef: [Author and Title](#)

Google Scholar: [Author Only](#) [Title Only](#) [Author and Title](#)

Tang J, Chu C. 2017. MicroRNAs in crop improvement: fine-tuners for complex traits. *Nature Plants* 3: 17077.

Pubmed: [Author and Title](#)

CrossRef: [Author and Title](#)

Google Scholar: [Author Only](#) [Title Only](#) [Author and Title](#)

Tong H, Chu C. 2009. Roles of DLT in fine modulation on brassinosteroid response in rice. *Plant signaling & behavior* 4: 438-439.

Pubmed: [Author and Title](#)

CrossRef: [Author and Title](#)

Google Scholar: [Author Only](#) [Title Only](#) [Author and Title](#)

Tong H, Chu C. 2016. Reply: Brassinosteroid regulates gibberellin synthesis to promote cell elongation in rice: critical comments on ross and quitteden's letter. *Plant Cell* 28: 833-835.

Pubmed: [Author and Title](#)

CrossRef: [Author and Title](#)

Google Scholar: [Author Only](#) [Title Only](#) [Author and Title](#)

Tong H, Jin Y, Liu W, Li F, Fang J, Yin Y, Qian Q, Zhu L, Chu C. 2009. DWARF AND LOW-TILLERING, a new member of the GRAS family, plays positive roles in brassinosteroid signaling in rice. *Plant Journal* 58: 803-816.

Pubmed: [Author and Title](#)

CrossRef: [Author and Title](#)

Google Scholar: [Author Only](#) [Title Only](#) [Author and Title](#)

Tong H, Liu L, Jin Y, Du L, Yin Y, Qian Q, Zhu L, Chu C. 2012. DWARF AND LOW-TILLERING acts as a direct downstream target of a GSK3/SHAGGY-Like kinase to mediate brassinosteroid responses in rice. *Plant Cell* 24: 2562-2577.

Pubmed: [Author and Title](#)

CrossRef: [Author and Title](#)

Google Scholar: [Author Only](#) [Title Only](#) [Author and Title](#)

Tong H, Xiao Y, Liu D, Gao S, Liu L, Yin Y, Jin Y, Qian Q, Chu C. 2014. Brassinosteroid regulates cell elongation by modulating gibberellin metabolism in rice. *Plant Cell* 26: 4376-4393.

Pubmed: [Author and Title](#)

CrossRef: [Author and Title](#)

Google Scholar: [Author Only](#) [Title Only](#) [Author and Title](#)

Ueguchi-Tanaka M, Nakajima M, Katoh E, Ohmiya H, Asano K, Saji S, Xiang HY, Ashikari M, Kitano H, Yamaguchi I, et al. 2007. Molecular interactions of a soluble gibberellin receptor, GID1, with a rice DELLA protein, SLR1, and gibberellin. *Plant Cell* 19: 2140-2155.

Pubmed: [Author and Title](#)

CrossRef: [Author and Title](#)

Google Scholar: [Author Only](#) [Title Only](#) [Author and Title](#)

Unterholzner SJ, Rozhon W, Papacek M, Ciomas J, Lange T, Kugler KG, Mayer KF, Sieberer T, Poppenberger B. 2015. Brassinosteroids are master regulators of gibberellin biosynthesis in Arabidopsis. *Plant Cell* 27: 2261-2272.

Pubmed: [Author and Title](#)

CrossRef: [Author and Title](#)

Google Scholar: [Author Only](#) [Title Only](#) [Author and Title](#)

Unterholzner SJ, Rozhon W, Poppenberger B. 2016. Reply: Interaction between Brassinosteroids and Gibberellins: Synthesis or Signaling? In Arabidopsis, Both! *Plant Cell* 28: 836-839.

Pubmed: [Author and Title](#)

CrossRef: [Author and Title](#)

Google Scholar: [Author Only](#) [Title Only](#) [Author and Title](#)

Van der Knaap E, Kim JH, Kende H. 2000. A novel gibberellin-induced gene from rice and its potential regulatory role in stem growth. *Plant Physiology* 122: 695-704.

Pubmed: [Author and Title](#)

CrossRef: [Author and Title](#)

Google Scholar: [Author Only](#) [Title Only](#) [Author and Title](#)

Vriet C, Russinova E, Reuzeau C. 2013. From Squalene to Brassinolide: The Steroid Metabolic and Signaling Pathways across the Plant Kingdom. *Molecular Plant* 6: 1738-1757.

Pubmed: [Author and Title](#)

CrossRef: [Author and Title](#)

Google Scholar: [Author Only](#) [Title Only](#) [Author and Title](#)

Wada K, Marumo S, Ikekawa N, Morisaki M, Mori K. 1981. Brassinolide and homobrassinolide promotion of lamina inclination of rice seedlings. *Plant and Cell Physiology* 22: 323-325.

Pubmed: [Author and Title](#)

CrossRef: [Author and Title](#)
Google Scholar: [Author Only Title Only Author and Title](#)

Wang L, Xu Y, Zhang C, Ma Q, Joo SH, Kim SK, Xu Z, Chong K. 2008. OsLIC, a novel CCCH-type zinc finger protein with transcription activation, mediates rice architecture via brassinosteroids signaling. PLoS One 3: e3521.

Pubmed: [Author and Title](#)
CrossRef: [Author and Title](#)
Google Scholar: [Author Only Title Only Author and Title](#)

Wu L, Zhang Q, Zhou H, Ni F, Wu X, Qi Y. 2009. Rice MicroRNA effector complexes and targets. Plant Cell 21: 3421-3435.

Pubmed: [Author and Title](#)
CrossRef: [Author and Title](#)
Google Scholar: [Author Only Title Only Author and Title](#)

Wu Z, Xu K, Zhao Y, He X, Wang X, Ling F. 2007. Changes of some agronomic traits in japonica Rice varieties during forty-seven years of genetic improvement in Jilin Province, China. Chinese Journal of Rice Science 21: 507-512.

Pubmed: [Author and Title](#)
CrossRef: [Author and Title](#)
Google Scholar: [Author Only Title Only Author and Title](#)

Yamamoto C, Ihara Y, Wu X, Noguchi T, Fujioka S, Takatsuto S, Ashikari M, Kitano H, Matsuoka M. 2000. Loss of function of a rice brassinosteroid insensitive1 homolog prevents internode elongation and bending of the lamina joint. Plant Cell 12: 1591-1605.

Pubmed: [Author and Title](#)
CrossRef: [Author and Title](#)
Google Scholar: [Author Only Title Only Author and Title](#)

Yang C, Shen W, He Y, Tian Z, Li J. 2016. OVATE Family Protein 8 positively mediates brassinosteroid signaling through interacting with the GSK3-like Kinase in rice. PLoS Genetics 12: e1006118.

Pubmed: [Author and Title](#)
CrossRef: [Author and Title](#)
Google Scholar: [Author Only Title Only Author and Title](#)

Yang J, Wang P, Liu L, Wang Z, Zhu Q. 2006. Evolution characteristics of grain yield and plant type for mid-season indica rice cultivars. Acta Agronomica Sinica 32: 949-955.

Pubmed: [Author and Title](#)
CrossRef: [Author and Title](#)
Google Scholar: [Author Only Title Only Author and Title](#)

Yuan, L. 2001. Breeding of super hybrid rice. In: Peng, S., Hardy, B. (Eds.), Rice Research for Food Security and Poverty Alleviation. International Rice Research Institute, Los Baños, Philippines, pp. 143-149.

Pubmed: [Author and Title](#)
CrossRef: [Author and Title](#)
Google Scholar: [Author Only Title Only Author and Title](#)

Zhang C, Bai MY, Chong K. 2014. Brassinosteroid-mediated regulation of agronomic traits in rice. Plant Cell Reports 33: 683-696.

Pubmed: [Author and Title](#)
CrossRef: [Author and Title](#)
Google Scholar: [Author Only Title Only Author and Title](#)

Zhang C, Xu Y, Guo S, Zhu J, Huan Q, Liu H, Wang L, Luo G, Wang X, Chong K. 2012. Dynamics of brassinosteroid response modulated by negative regulator LIC in rice. PLoS Genetics 8: e1002686.

Pubmed: [Author and Title](#)
CrossRef: [Author and Title](#)
Google Scholar: [Author Only Title Only Author and Title](#)

Zhang LY, Bai MY, Wu JX, Zhu JY, Wang H, Zhang ZG, Wang WF, Sun Y, Zhao J, Sun XH, et al. 2009. Antagonistic HLH/bHLH transcription factors mediate brassinosteroid regulation of cell elongation and plant development in rice and Arabidopsis. Plant Cell 21: 3767-3780.

Pubmed: [Author and Title](#)
CrossRef: [Author and Title](#)
Google Scholar: [Author Only Title Only Author and Title](#)

Zong Y, Wang Y, Li C, Zhang R, Chen K, Ran Y, Qiu JL, Wang D, Gao C. 2017. Precise base editing in rice, wheat and maize with a Cas9-cytidine deaminase fusion. Nat Biotechnol. 35: 438-440.

Pubmed: [Author and Title](#)
CrossRef: [Author and Title](#)
Google Scholar: [Author Only Title Only Author and Title](#)